Model Studies of Ferulate-Coniferyl Alcohol Cross Products Formed in Primary Maize Walls

J.H. Grabber, J. Ralph and R.D. Hatfield

Introduction

During cell-wall biosynthesis in grasses, feruloylated xylans become extensively cross-linked by coupling of ferulate into diferulates (Fig. 1) and by copolymerization ferulate and diferulate xylan esters with monolignols to form xylan-lignin complexes. As demonstrated in earlier studies, nonlignified primary walls isolated from maize cell suspensions are a valuable model system for studying the dimerization of ferulates and their subsequent incorporation into lignin. In the current study, this system was used to characterize the types of cross-products formed between ferulates and coniferyl alcohol (**3**). Coniferyl alcohol, with or without *p*-coumaryl and sinapyl alcohols, is the most abundant and consistently observed monolignol secreted into cell walls at the onset of lignification.

Methods

Cell walls from maize cell suspensions were treated with dilute hydrogen peroxide to dimerize ferulate via wall bound peroxidase. These walls, containing 52 mmol g^{-1} of ferulate monomers and 33 mmol g^{-1} of diferulates, were then partially lignified with 110 mmol g^{-1} of coniferyl alcohol for subsequent identification of ferulate- and diferulate-lignin cross-products in alkaline hydrolysates by GC-MS and NMR.

Results and Discussion

Alkaline hydrolysis and GC-FID analysis revealed that about 50% of the total ferulate in walls (11.8 mg g^{-1}, 47 mmol) copolymerized with about 19 mg g^{-1} (105 mmol) of coniferyl alcohol. As noted previously, ferulate and 5–5-coupled diferulate had the greatest propensity to copolymerize with coniferyl alcohol, accounting for 82% of the cross-coupled structures formed. GC-MS analysis revealed that ferulate monomers were coupled to coniferyl alcohol by 8-β', 5-β', 4-*O*-β' linkages (Fig. 2 and 3). Coupling of ferulate to the β'-position of coniferyl alcohol suggests that ferulate can act as a nucleation site where lignification begins. The observed 8-β' product **18** was probably present in the walls as **15** with structure **18** being formed during saponification and acidification. Based on GC analysis, 4-*O*-β', 8-β', and 5-β' structures comprised about 52, 35, and 13% of the dimeric cross-products recovered from cell walls. If these proportions are representative of grass cell walls, then substantial amounts ferulate-mediated cross-links between xylans and lignin could be lost via de-esterification if **18** was the major product of 8-β' coupling. As a result, oxidative coupling of ferulate into 8–8-, 8–5-, and 8–*O*–4-coupled diferulates takes on added importance; these dimers not only mediate cross-linking among xylans and between xylans and lignin, their lack of 8-β'-coupling with monolignols precludes the loss of cross-links via this pathway. In addition to 4-*O*-β', 8-β', and

5-β' cross-products, minor correlations of 8–*O*–4'- and 8–5'-coupled cross-products were detected by HMBC-NMR (Fig. 4), indicating that some ferulate or 5–5-coupled diferulate coupled with dimers or oligomers of coniferyl alcohol. Coupling of ferulate with lignin oligomers suggests that ferulates do not act solely as nucleation sites for lignin formation.

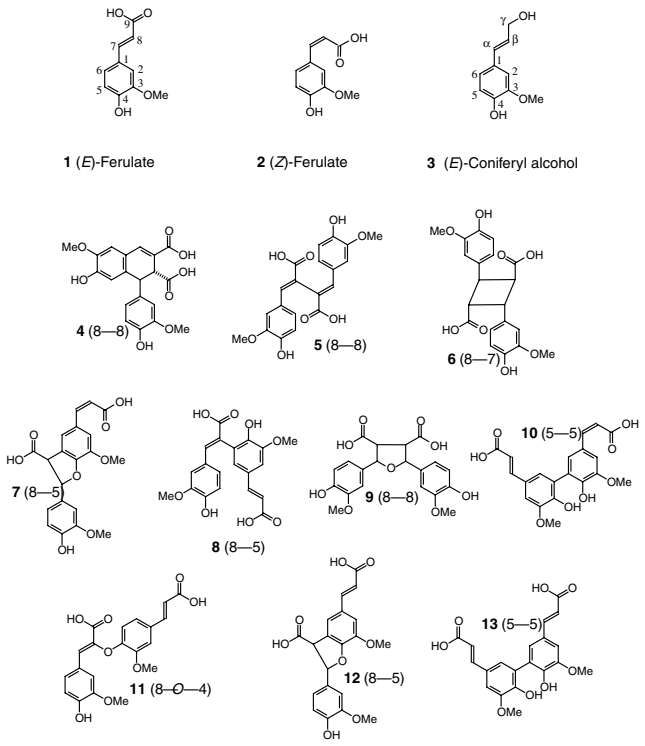

Fig. 1. Ferulates (**1**, **2**) and diferulates (**4**-**13**) released from primary walls of maize by alkaline hydrolysis. Ferulate xylan esters and coniferyl alcohol (**3**) may undergo oxidative coupling at the 8- or β-, 5- and 4–*O*-positions. Diferulate esters may undergo oxidative coupling with monolignols at their 5- and 4–*O*-positions; only 5–5-coupled diferulate has the potential to couple with monolignols at its 8-position.

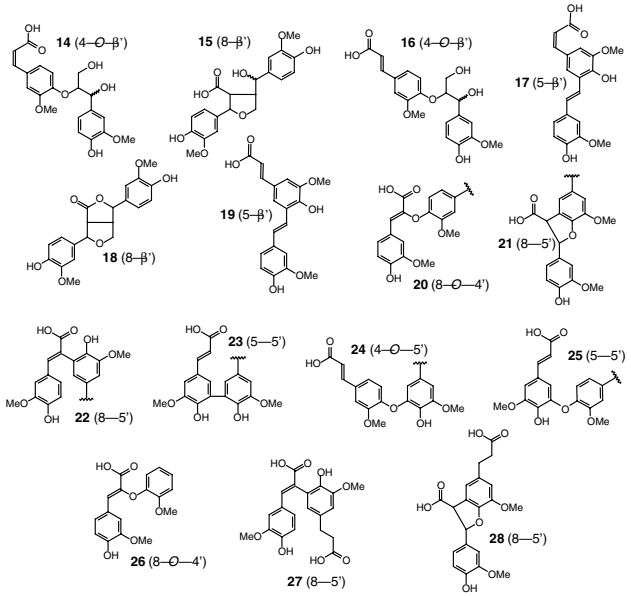

Fig. 2. Potential cross-products between ferulate and coniferyl alcohol released by saponification of cell walls (**14**-**25**). Diferulates can form similar types of cross-products with coniferyl alcohol. Several cross-product models (**26**-**28**) were prepared for NMR studies.

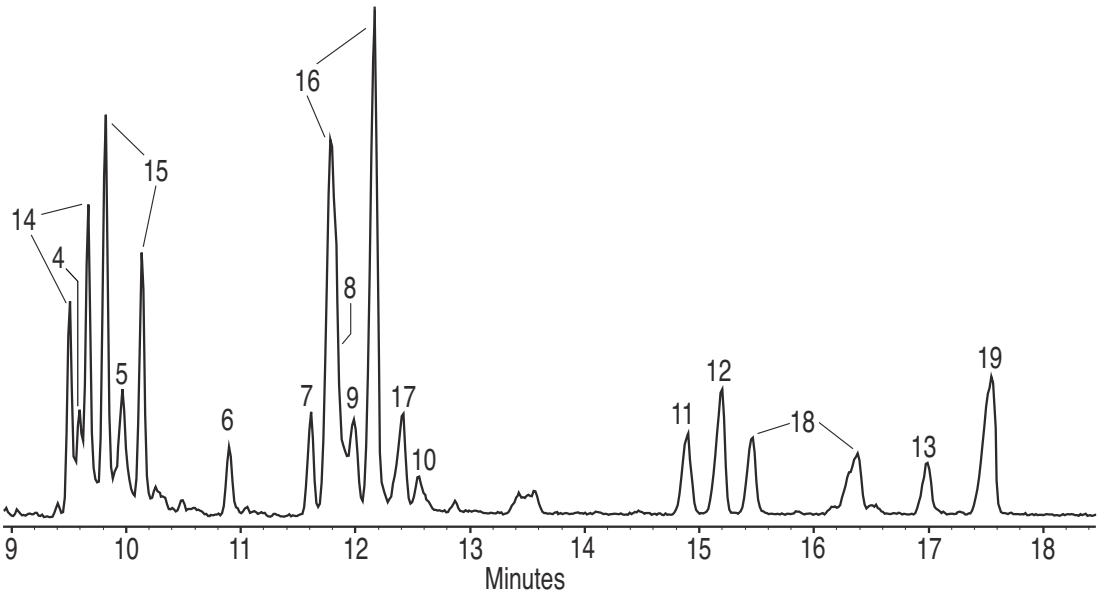

Fig. 3. GC-MS total ion chromatogram of diferulates and ferulate-coniferyl alcohol dimers recovered following room-temperature alkaline hydrolysis of partially-lignified primary walls from maize suspension cultures.

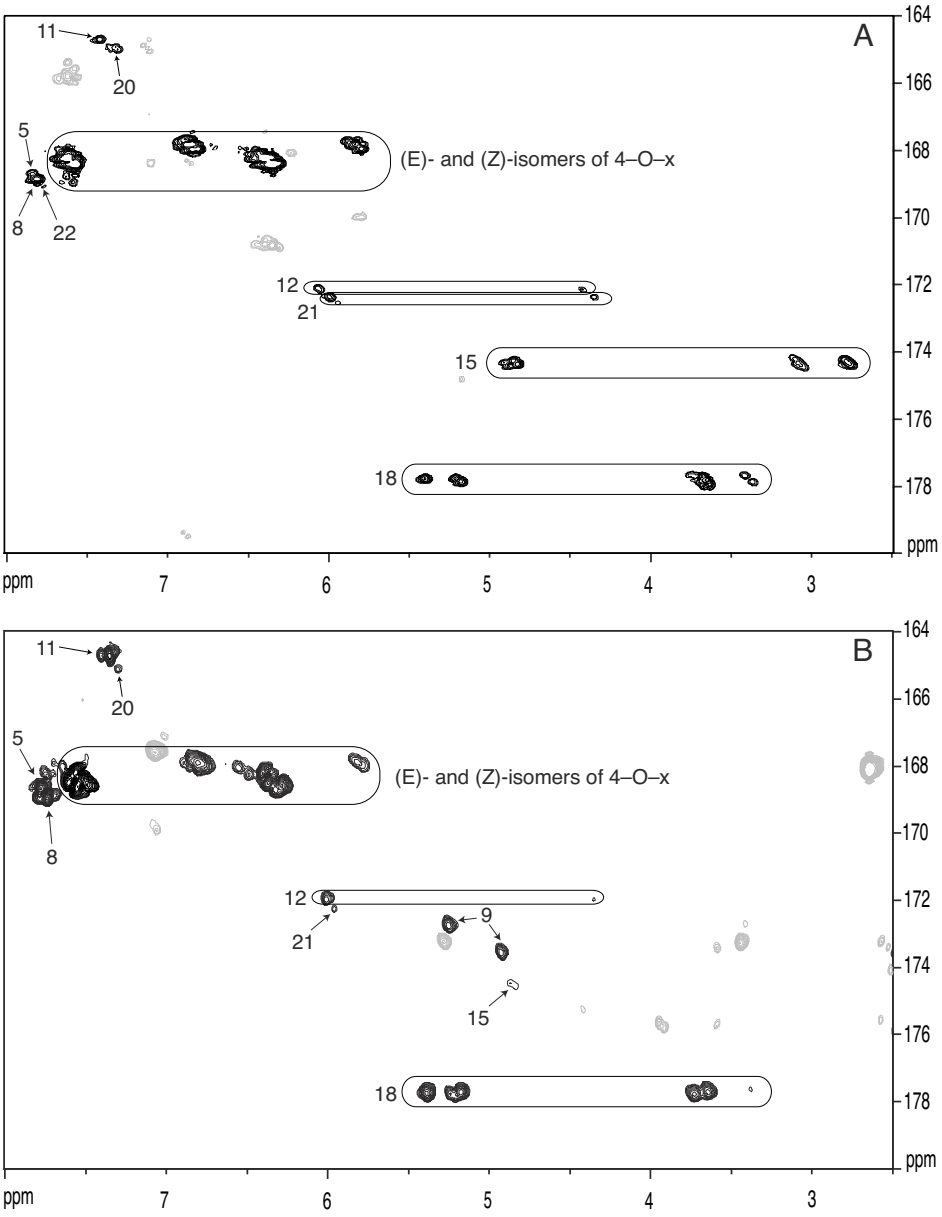

Fig. 4. Long-range C-H correlation (HMBC) spectra of ferulate, diferulates, and their cross-products recovered following room-temperature alkaline hydrolysis of partially-lignified primary walls from maize suspension cultures. (A) Fraction 1 recovered by EtOAc extraction (B) Fraction 2 recovered from the $MgSO_4$ used to dehydrate the EtOAc extract.

Cross-Products Between Ferulate and Coniferyl Alcohol Act as Nucleation Sites for Lignin Formation in Primary Maize Walls

J.H. Grabber, J. Ralph and R.D. Hatfield

Introduction

Ferulate-xylan esters may act as initiation or nucleation sites for lignin formation in grasses—the site at which lignification begins in cell walls. Our group obtained the first evidence for this in HMBC-NMR studies of ^{13}C-labeled ryegrass lignin; initial coupling reactions exclusively involved ferulate coupled to the β-position of monolignols. The milled "wood" lignin isolated from ryegrass was likely derived from secondary cell walls, whereas lignification in grasses starts in the middle lamella and primary cell wall. Consequently, we know little about the role of ferulates as nucleation sites where lignification begins in cell walls.

Methods

A dilute H_2O_2 solution was added to primary walls isolated from maize cell suspension to stimulate oxidative coupling of ferulate into diferulates by wall bound peroxidase. Walls were then slowly lignified *in situ* by adding solutions of coniferyl alcohol and H_2O_2. Samples were analyzed for Klason lignin and for alkali-labile ferulates and diferulates by GC-FID.

Results and Discussion

Primary maize walls were lignified with varying levels of coniferyl alcohol to study the incorporation of ferulate and diferulate isomers into lignin and the growth of ferulate/diferulate-lignin complexes. For our purposes, the ferulate and diferulate isomers were combined into two functional groups—ferulate/5–5-coupled diferulate and 8-coupled diferulates—based on their kinetics of incorporation into lignin. Coniferyl alcohol was efficiently polymerized into cell walls, forming cross-coupled structures with up to 95% of the ferulates and diferulates in cell walls (Fig. 1a). Ferulate and diferulates incorporated as at least two pools with the larger pool incorporating earlier and more rapidly than the smaller pool. Incorporation of the larger pool was 3.5-fold faster for ferulate/5–5-coupled diferulate than for 8-coupled diferulates, confirming previous observations that initial cross-coupling reactions with monolignols overwhelmingly involve ferulate and 5–5-coupled diferulate. During lignification, the size of complexes increased linearly even as the incorporation of total ferulates per unit coniferyl alcohol declined dramatically (Fig1b). As illustrated in Figure 2, this suggests that cross-products between coniferyl alcohol and ferulate/5–5-coupled diferulate, formed at the onset of lignification, act as preferred sites for continued lignin polymerization. Preferential growth of lignin at these sites occurred although more numerous non-incorporated ferulates and diferulates were available for cross-coupling with coniferyl alcohol. Our group is currently conducting additional model studies with maize walls and investigating means of isolating additional lignin from the ^{13}C-labelled ryegrass, in order to more definitively establish whether ferulates act as nucleation sites for lignin formation in grasses.

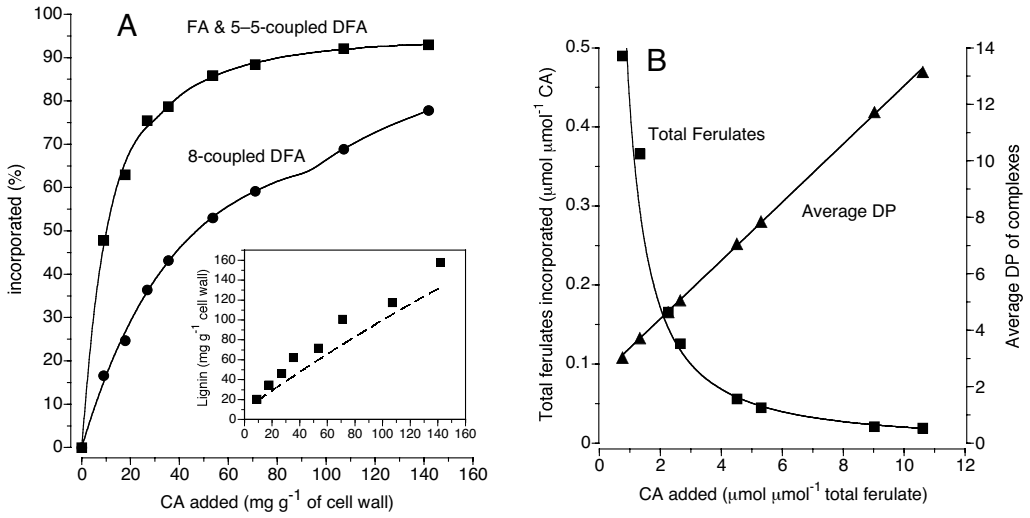

Fig. 1. (A) Incorporation of Ferulate (FA) and 5–5-coupled diferulate (DFA) and of 8-coupled DFA during lignification of primary maize walls with coniferyl alcohol (CA). The insert shows the Klason lignin content of walls compared to the predicted lignin content of walls with complete incorporation of CA (dashed line). (B) Comparison of the incorporation of total ferulates (ferulate monomers plus dimers) with the apparent degree of polymerization (DP) of complexes formed between total ferulates and CA.

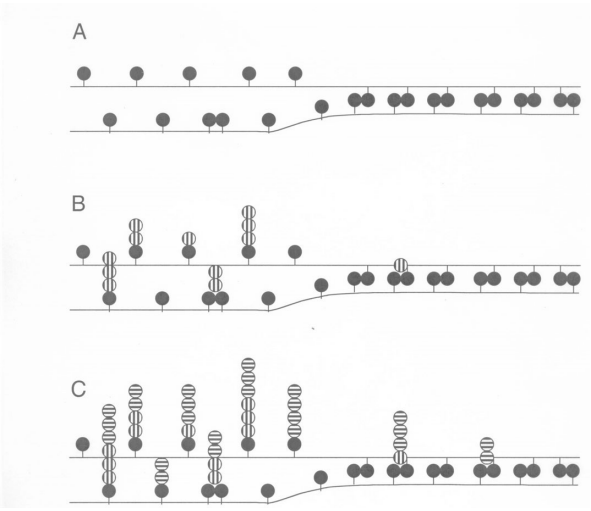

Figure 2. A schematic drawing illustrating the role of cross-products between ferulate/5-5-coupled diferulate and coniferyl alcohol as nucleation sites for continued lignin formation. (A) Non lignified walls with xylans substituted with ferulate and cross-linked with diferulates (solid circles). (B) At the onset of lignification, coniferyl alcohol (circles with vertical stripes) couples mainly with ferulate monomers, 5-5-coupled diferulate, and their cross-products. (C) As lignification continues, additional coniferyl alcohol (circles with horizontal stripes) preferentially couples with existing cross-products, even though unincorporated ferulate monomers, 5-5-coupled diferulate, and particularly 8-coupled diferulates predominate as potential coupling sites.

Relationship of Growth Cessation with the Formation of Diferulate Cross-Links and *p*-Coumaroylated Lignins in Tall Fescue Leaf Blades

J.W. MacAdam and J.H. Grabber

Introduction

The discovery of 5–5-coupled diferulic acid linkages between adjacent feruloylated xylan chains led to the hypothesis that such bonds control cell wall extensibility and tissue growth in grasses. Numerous studies have demonstrated a correlation between an increase in the content of 5–5-coupled diferulic acid in cell walls of coleoptiles and a decrease in growth and cell wall extensibility. The 5–5-coupled dimer, however, represents only a small portion of the total diferulates in grass walls. In addition, 5–5-coupled diferulate (unlike 8-coupled diferulates) is probably formed by intramolecular dimerization of ferulate polysaccharide esters. Therefore, most if not all cross-linking mediated by ferulic acid involves 8–*O*–4, 8–8-, and 8–5-coupled diferulates, yet relationships between 8-coupled diferulates and cell wall extension have been ignored, even in recent studies with cereal coleoptiles. Lignification of primary walls has also been associated with reduced extensibility and growth of coleoptiles. Although very small quantities of *p*-coumarate are esterified to arabinoxylans, most *p*-coumarate deposition occurs in tandem with lignification, making *p*-coumarate accumulation a convenient indicator of lignification. In previous work, we observed that the elongation rate of tall fescue leaf blades increased exponentially and then stopped abruptly, implying a rapid change in cell wall mechanical properties. Therefore, the main objective of this study was to investigate relationships between the cell-wall deposition of ferulate monomers, all major diferulates, and *p*-coumarate with changes in the segmental elongation rate of tall fescue leaf blades.

Materials and Methods

Vegetatively propagated tillers of tall fescue with high and low leaf elongation rates (LER) were grown in a controlled environment chamber. Prior to sampling, mean daily elongation rates were calculated by measuring the length of nine leaves over a 5-d period following leaf emergence. At the time of destructive sampling, epidermal cell lengths were measured from Formvar replicas prepared from the abaxial surface of leaf blades. Segmental elongation rates (SER) were calculated from leaf elongation rates and cell length profiles. The time of maximal SER was estimated by solving a quadratic equation fit through SER data points. The time at which SER transitioned from an increasing rate of increase to a declining rate of increase was estimated by solving a quadratic equation fit through the first derivative of SER points. The first derivative of each point of the SER curve was calculated by fitting a quadratic equation through that point and its nearest neighbors. Cell walls isolated from 5-mm segments cut from leaf blades were analyzed for alkali-labile *p*-hydroxycinnamates by GC-FID. A segmented quadratic-plateau regression model was used to estimate the time at which the deposition of *p*-hydroxycinnamates began during leaf development.

Results and Discussion

Leaf elongation rate averaged 1.35 mm h^{-1} for the high-LER genotype and 0.54 mm h^{-1} for the low-LER genotype. The length of the elongation zone, determined from cell length profiles, was about 22 mm for both genotypes. Residence time of epidermal cells in the meristem and elongation zones averaged 140 h for the high-LER genotype and 400 h for the low-LER genotype. SER of both genotypes initially increased at an increasing rate and then transitioned to a declining rate of increase

at about -21 h (time to cessation of elongation) in the high-LER genotype and at about -52 h in the low-LER genotype (Fig. 1). SER reached a maximum of 0.089 mm/mm/h at about -11 h in the high-LER genotype and 0.036 mm/mm/h at about -28 h in the low-LER genotype. After reaching a maximum, SER declined rapidly as epidermal cells stopped elongating.

Accretion of ferulate and diferulates in cell walls of high-LER leaf blades began about 23 h before elongation stopped (Fig. 1a). In the low-LER genotype, ferulate accretion began about 67 h before elongation ceased (Fig. 1b). The accumulation of diferulic acids in the low-LER genotype was delayed, beginning about 14 h later; the expanded time frame of low-LER elongation allowed a better separation of the data for deposition of these two cell wall components. In both genotypes, deposition of diferulates into cell walls began within 1 or 2 h of the time when SER transitioned from an increasing to a declining rate of increase. During growth of the high LER genotype, concentrations of 8–5- and 8–*O*–4-coupled isomers increased 10-fold from -20 to +20 h from cessation of elongation (Fig. 2a), Concentrations of 8–8- and 5–5-coupled isomers increased only 5-fold over the same 40 h period. Similar changes in diferulate concentrations were apparent from -50 to +50 h for the low-LER genotype (Fig 2b). The 5–5-coupled dimer comprised only a small and variable proportion (12-17%) of the total diferulates in cell walls, making it a poor indicator of diferulate cross-linking in developing leaf blades.

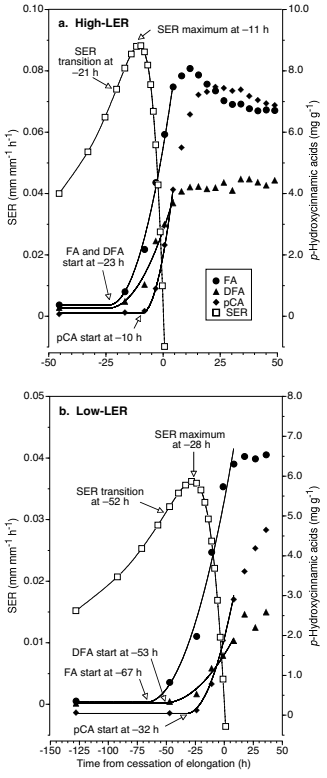

The deposition of *p*-coumarate occurred later in leaf development, beginning about 10 and 32 h before elongation ceased in the high- and low-LER genotypes, respectively (Fig. 1). Accretion of *p*-coumarate, and therefore of *p*-coumaroylated lignins, began just before or at the time when SER reached a maximum and then rapidly declined to zero. These results, using genotypes with differing growth characteristics, suggest that leaf elongation is slowed somewhat at the onset of diferulate cross-linking and ended by the deposition of *p*-coumaroylated lignin in cell walls. The role of ferulate cross-linking in halting growth may, however, be greater than indicated by this analysis since incorporation of ferulate and diferulate xylan esters into lignin dramatically increases ferulate mediated cross-linking of cell walls. Indeed this type of cross-linking may represent a primary mechanism by which lignin reduces cell wall extensibility. The temporal association of ferulate cross-linking and *p*-coumaroylated lignin deposition with growth cessation does not, however, demonstrate a cause and effect relationship. Further work is underway to clearly demonstrate whether ferulate cross-linking and lignification are mechanisms by which growth is stopped in grasses.

Fig. 1 Segmental elongation rate (SER) and cell-wall concentrations of ferulate (FA), diferulates (DFA), and *p*-coumarate (pCA) in leaf blades from the (a) high-LER and (b) low-LER genotypes of tall fescue. The segmented curves used to predict the start times of *p*-hydroxycinnamate accretion are indicated on the figure.

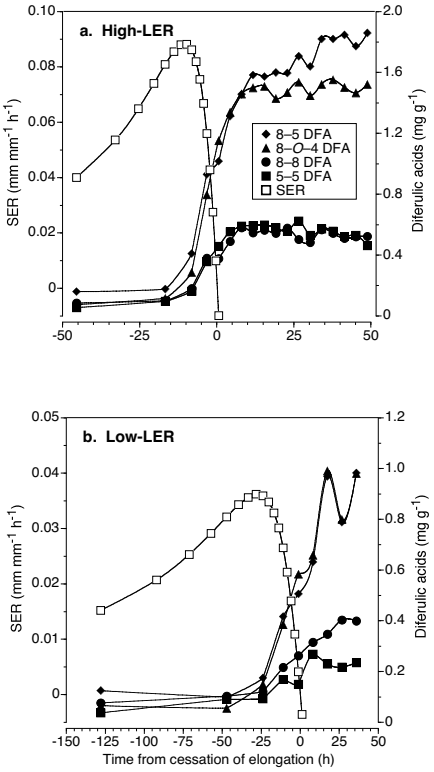

Fig. 2 Segmental elongation rates (SER) and cell-wall concentrations of diferulate (DFA) isomers in leaf blades of the (a) high-LER and (b) low-LER genotype of tall fescue

Deposition of *p*-Hydroxycinnamates Into Fescue Leaf Blades During Primary and Secondary Cell Wall Development

J.H. Grabber and J.W. MacAdam

Introduction

Ferulates are esterified to α-L-arabinose sidechains on xylans in grasses. During wall biosynthesis and lignification, xylans are cross-linked by oxidative coupling of ferulate monomers into dehydrodimers. During lignification, ferulate and diferulate esters copolymerize with monolignols, thereby cross-linking xylans to lignin. These cross-links probably contribute to wall stiffening and growth cessation in grasses and to poor degradation of grass walls by hydrolytic enzymes. The fate of ferulate and diferulates in walls are difficult to track because ferulate deposition, dimerization, and copolymerization into lignin are overlapping processes during cell wall formation in grasses. This difficulty is further compounded by our inability to fully recover or characterize, by solvolytic or spectroscopic methods, ferulates in lignified walls. In previous studies, cell-wall concentrations of ferulate were reported to decline during secondary wall formation in grass tissues. This reduction in *measurable* ferulate during secondary wall formation has been used to support the contention that most ferulates are deposited in primary cell walls. The current study with tall fescue leaves provides evidence that most ferulate and diferulate accretion occurs during secondary cell wall formation. The accretion of *p*-coumarate was also examined in relation to cell wall deposition.

Materials and Methods

Vegetatively propagated tillers of high and low leaf elongation rate (LER) genotypes of tall fescue were grown in a controlled environment chamber. Prior to sampling, mean daily elongation rates were calculated by measuring the length of nine leaves over a 5-d period following leaf emergence. At the time of destructive sampling, epidermal cell lengths were measured from Formvar replicas prepared from the abaxial surface of leaf blades. Segmental elongation rates (SER) were calculated from leaf elongation rates and cell length profiles. The time of maximal SER and minimal cell wall mass were estimated by solving a quadratic equation fit through data points. Cell walls isolated from 5-mm segments cut from leaf blades were analyzed for alkali-labile *p*-hydroxycinnamates by GC-FID. A segmented quadratic-plateau regression model was used to estimate the time at which the deposition of cell walls and *p*-hydroxycinnamates ended during leaf development.

Results and Discussion

Cell wall mass initially decreased toward the distal end of the elongation zone with water uptake and cell expansion (Fig. 1), reaching a minimum within a few hours after cell elongation stopped in leaves. Cell wall mass then increased, due to secondary cell wall deposition, ending about 46 h after elongation ceased.

When plotted on a mg mm^{-1} basis, it is clear that the deposition of ferulate and particularly diferulates continued into the later stages of secondary cell wall formation (Fig. 2). Based on our data, at least 70% of *measurable* alkali-labile total ferulates (monomers and dimers) were deposited during secondary wall formation. The concentration of *p*-coumarate appeared to plateau about 33 h after elongation ceased, about 13 h before secondary cell wall deposition ended. Although the dataset for the low-LER genotype is less complete, similar patterns of ferulate, diferulates, and *p*-coumarate deposition during cell wall formation were apparent (data not shown).

Our analyses, however, underestimate the concentrations of ferulate and diferulates in more mature tissues because ferulate and diferulates readily copolymerize into lignin. Once incorporated into lignin, ferulate and diferulates are not released from lignin by room temperature alkaline hydrolysis. Indeed, most ferulate- and diferulates-lignin cross-links are not cleaved even by high-temperature alkaline hydrolysis or by other solvolytic methods currently used to estimate such cross-linking in cell walls. Therefore, researchers should exercise caution when relating ferulate or diferulate concentrations to cell-wall deposition, extensibility, or growth when lignification of tissues has commenced.

Since *p*-coumarate is primarily a component of lignin, these observations may indicate that lignification stops before secondary wall formation is completed. An alternative interpretation is that acylation of monolignols by *p*-coumarate slows or stops at the latter stages of lignification. In contrast to ferulate, *p*-coumarate esters on lignin units form few, if any, cross-linked structures mediated by radical coupling reactions. *p*-Coumarate (and ferulate) can, however, undergo a photocatalyzed cyclodimerization during tissue development to form truxillic and truxinic acids but none were detected by GC-FID. Therefore, room-temperature alkaline hydrolysis, as used in this study, provides a good estimate of the total quantity of *p*-coumarate in walls.

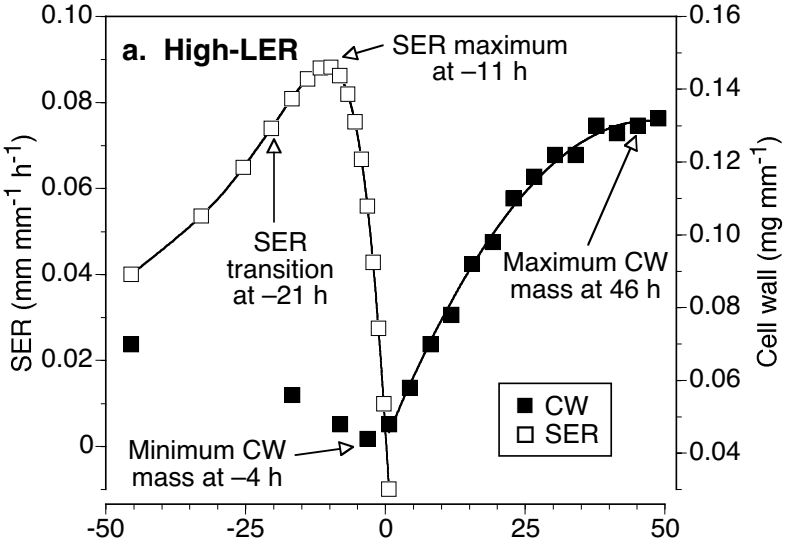

Fig. 1. Segmental elongation rates (SER) and mass of cell walls (CW) of leaf blades from the high-LER genotype of tall fescue. Data are plotted at the centers of 5-mm-long leaf blade segments. The segmented curves used to predict the time of maximum CW accretion are indicated on the figure.

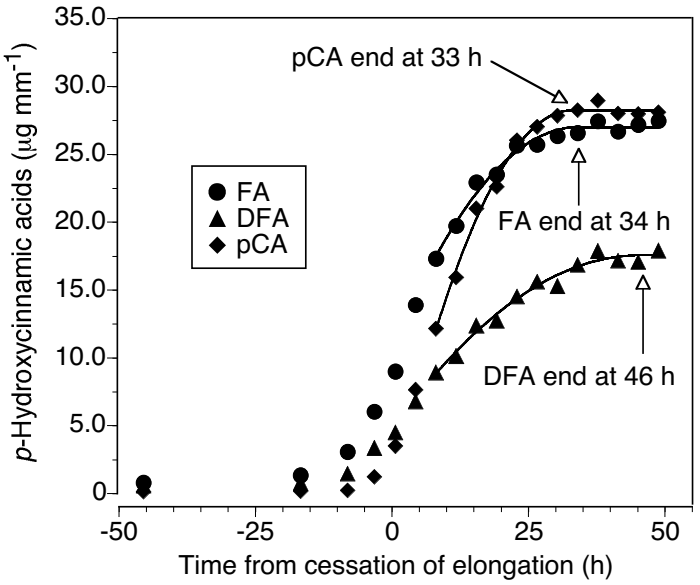

Fig. 2. Per-unit-length contents of ferulate (FA), diferulates (DFA), and *p*-coumarate (pCA) in leaf blades from the high-LER genotype of tall fescue. The segmented curves used to predict the end of *p*-hydroxycinnamate accretion are indicated on the figure.

Diferulates Analysis: Diferulates and Disinapates in Insoluble Cereal Fiber

M. Bunzel, John Ralph, J.M. Marita, F. Lu, R.D. Hatfield, H. Kim, J.H. Grabber, S.A. Ralph, G. Jiminez-Monteon, and H. Steinhart.

Introduction

Grasses have substantial amounts of hydroxycinnamic acids intimately associated with the cell wall. Ferulate, in particular, has a significant role in cross-linking. Polysaccharide-polysaccharide cross-linking is achieved by ferulate dehydrodimerization by either photochemical or, more importantly, radical coupling reactions of ferulate-polysaccharide esters. The whole range of ferulate dimers **1**-**9**, Fig. 1, are now routinely being found in a variety of samples. Radical cross-coupling of (polysaccharide-linked) ferulates with lignin monomers results in lignin-polysaccharide cross-linking. Even ferulate dimers cross-couple with lignin monomers/oligomers to incorporate into the lignin polymer resulting in extensive polysaccharide-polysaccharide-lignin cross-linking.

Methods of Analysis

Although HPLC methods have been used for qualitative and quantitative analysis of diferulates, HPLC really cannot afford the dispersion and resolution of GC. In addition, alkaline hydrolysates of plant materials produce a wide range of products that cannot be easily pre-fractionated. For example in grass stem samples, in addition to the diferulates from radical coupling of ferulates are the photochemical dimers and numerous ferulate-monolignol crossed dimers. There are many components still to be identified. As indicated below, two new diferulates have recently been found, along with dimers of another hydroxycinnamate, sinapate. Only cursory analyses are currently possible using HPLC; GC-FID and/or GC-MS should be used if component detail is required.

Mass spectral data for the diferulates have been requested by many groups. Spectra from both a quadrapole EI instrument and an Ion Trap are given in Fig. 1. We have been impressed with the ion trap instrument for providing enhanced sensitivity in the high-mass region. The ion-trap spectra of all of the diferulates have a molecular ion peak that is quite abundant; quadrapole instruments tend to favor the uninformative trimethylsilyl peak at 73, and typically yield weak molecular ions.

A Better GC Standard for Diferulates Analyses

The standard used for the original quantification of diferulates and most subsequent studies has been *o*-coumaric acid. Unfortunately this standard has neither ideal elution nor satisfactory response factors for the diferulates. A standard having better structural similarity was sought. Rather extensive surveys failed to unearth a satisfactory commercially available standard. We decided that the 5–5-coupled dimer which had been monomethylated might be a good candidate, and this has been used in our labs. However, it was discovered somewhat late in the analysis process that the "standard""**IS** was contaminated with the di-methylated compound **IS*** (see the chromatograms in Fig. 2), from which separation was extremely difficult. We are now examining the use of the fully methylated dimer as well as seeking cleaner and simpler methods to prepare the monomethylated dimer. Our lab will eventually provide the chosen reference compound to other labs interested in using it.

Discovery of the Full Range of Ferulate Dimers (Diferulates)

The sole ferulic acid dehydrodimer reported from plant cell walls before 1994 was 5–5-diferulic acid **7**. The more recent determination (and authentication) of a range of diferulates from grasses stemmed from a recognition that radical coupling of ferulates, necessary to produce the 5–5-coupled dehydrodimer **7**, could produce other dehydrodimers by anticipated 8–5-, 8–8-, 8–O–4- and 4–O–5-coupling reactions, analogous to those observed for coniferyl alcohol during lignification. Unless the radical coupling was directly controlled by an enzyme or, as been more recently revealed in lignan biosynthesis, a dirigent protein other dimers would be expected to be more prevalent than the 5–5-dimer. This has been found to be the case in every plant material subsequently examined.

The only dehydrodimer not found until recently was 4–O–5-DFA–**9**, Fig. 1. This diferulic acid has also now been found (in rather small amounts) in several insoluble cereal fibers, as described in the following report ("Identification of the Last Elusive Diferulate Linkage"). The finding completes the spectrum of ferulate dehydrodimers to be found in plants, and supports the concept of free-radical coupling of cell wall components independently of enzymes or proteins which might otherwise confer a strict regiochemical course, i.e. produce only a single diferulate.

Another 8–8-coupled Diferulate?

Most alkaline hydrolysates of grass cell walls also contain another previously unidentified peak. MS analysis suggests that it is the tetrahyrdrofuran dimer **4**, Fig. 1. As can be seen in the chromatogram in Fig. 2, it is a substantial component that should also be quantified as resulting from 8–8-dimerization. Work is currently underway to isolate sufficient amounts of the compound for structural elucidation by NMR and to synthesize it.

Levels of Diferulates in Cereal Grain Insoluble Fiber

Grain fiber is known to be beneficial for human nutrition. The levels of diferulates in a range of cereal grain fibers was recently surveye: maize 12.6, wheat 2.4, spelt 2.6, rice 4.0, wild rice 2.8, barley 3.7, rye 4.0, oat 3.6 and millet 5.7 mg/g of insoluble fiber. Very low levels were found in the soluble fiber fraction as might be anticipated. The high levels in maize make this an ideal secondary standard to check column performance and variations in the analyses over longer periods of time.

Disinapates Cross-linking Cell Wall Polysaccharides??

Although sinapic acid has been identified in plant extracts and can be released in small quantities from grass cell walls by low-temperature base, it has not been determined if it acylates polysaccharides or other components. Nor has sinapate been shown to be involved in radical coupling reactions to produce dehydrodimers. Preliminary identification of such radical dehydrodimerization products in the insoluble fiber fraction from wild rice samples is presented here.

GC-MS total ion chromatograms of saponified extracts from wild rice (*Zizania palustris* L.) insoluble fiber showed additional peaks in the dimer region; two peaks were especially predominant. The mass spectra were analogous to those of ferulate dimers, with masses of various peaks offset by 30 or 60 mass units (corresponding to one or two additional methoxyls). The products could also be obtained by saponification of dimers prepared by oxidative coupling of ethyl sinapate. We assume

that they are the two 8–8-coupled disinapate analogs of the 8–8-diferulates **1** and **2**, one ring form and one open-chain. We are currently independently synthesizing both products to identify them conclusively.

Although it is logical that sinapoylated polysaccharides might be cross-linked by radical dimerization of the sinapates in an analogous way to the ferulates, we have not demonstrated that they are in fact esterified to polysaccharides. It is also curious that disinapates would form with little evidence (from MS data so far) of any cross-coupling products between ferulate and sinapate; however, we have not yet examined the propensity for such cross-coupling. If disinapates are found in cell wall fractions from stems or grains of plants other than wild rice, such issues should be clarified by further research.

Conclusions

Diferulates continue to emerge in varied roles as significant components of many plant fibers and have interesting implications for human and animal health as well as for their properties in limiting cell wall digestibility by ruminants. The 4–O–5-coupled dimer has now been found in small quantities in many cereal grains in which the insoluble fiber fraction contains high levels of total diferulates, up to 12.6 mg/g in maize. A new form of the 8–8-dimer (a tetrahydrofuran) has also been found. Many dimers of ferulate cross-coupled with monolignols (not detailed here) can also be found in grain and stem fibers. Sinapates in wild rice, like ferulates in all grasses, appear to dimerize via radical coupling reactions to produce at least two sinapate dehydrodimers, which can be detected by GC(-MS). We assume new roles for such hydroxycinnamate dehydrodimers will continue to be discovered and researchers will learn more about their impact on other physiological processes.

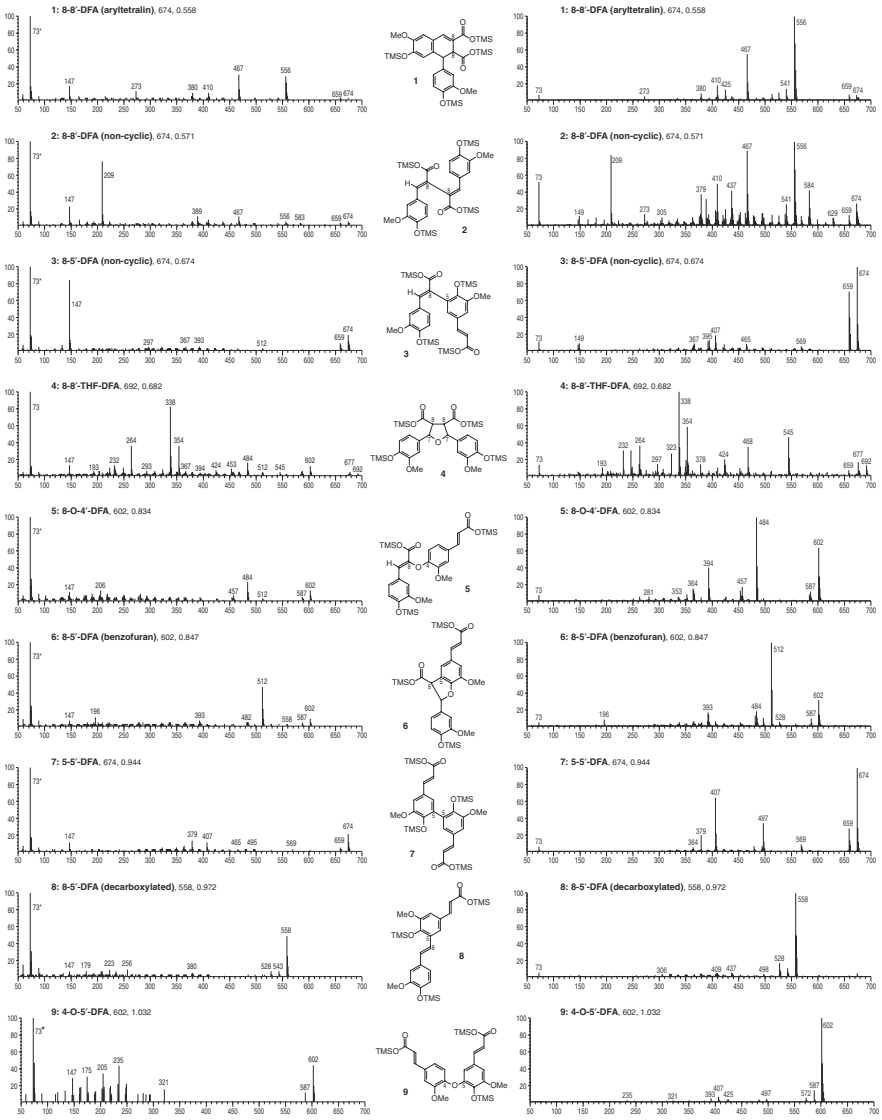

Fig. 1. Structures and mass spectra from the nine diferulate products resulting from saponification of cereal insoluble fiber. The left column of spectra are traditional EI spectra from an HP 5970 bench-top quadrapole instrument. Note that spectra in which the TMS peak is noted as 73* have had all peaks but the 73 peak doubled in intensity for easier viewing of the important high-mass peaks. The right column of spectra are from a Thermoquest Polaris GCQ ion-trap instrument, and generally show superior molecular ion peaks. Spectrum labels include, in addition to the compound number and name, the nominal mass and the retention time relative to **IS**, the monomethylated 5-5-coupled ferulate dimer.

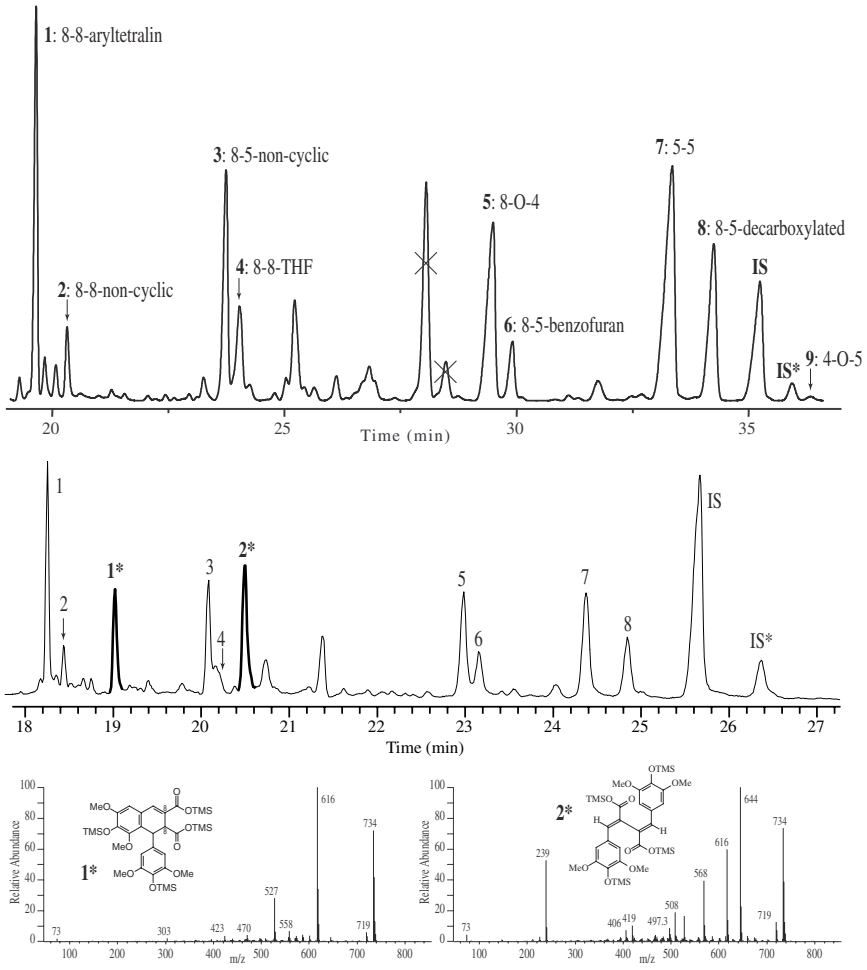

Fig. 2. *Top.* GC-MS total ion chromatogram of the dimers region from saponification of maize grain insoluble fiber showing diferulate products **1**-**9**. The crossed out peaks are apparently artifacts that are not present in more recent chromatograms from such samples. **IS** is the mono-methylated derivative of the 5–5-dimer **7**; the di-methylated derivative is also present, **IS***. *Middle.* Similar data (different machine and conditions!) for wild rice insoluble fiber hydrolysate showing diferulates and two new disinapates. *Bottom.* Ion-trap mass spectra of disinapates (structures to be confirmed).

Identification of the Last Elusive Diferulate Linkage

M. Bunzel, J. Ralph, J.M. Marita, G. Jimenez-Monteon, R.D. Hatfield and H. Steinhart

Introduction

Ferulates play an important role in modifying the mechanical properties of cell walls as well as in limiting polysaccharide degradation by exogenous enzymes by acting as cross-links between polysaccharides and between polysaccharides and lignin. Dimerization of ferulates is a mechanism for cross-linking cell wall polysaccharides.

The more recent determination of a range of diferulates from grasses stemmed from a recognition that radical coupling of ferulates, necessary to produce the 5-5 dehydrodimer, could produce other dehydrodimers by anticipated 8-5-, 8-8-, 8-O-4- and 4-O-5-coupling reactions. These other dimers have been found to be more prevalent than the 5-5-dimer in every plant material subsequently examined (see discussion section). Prior to this study, the only dehydrodimer *not* found was 4-O-5-DFA (Fig. 1). This paper reports its identification and semiquantitative determination in several insoluble cereal fibers.

Methods

Internal Standard (E,E)-4-hydroxy-4,5,5-trimethoxy-3,3-bicinnamic acid. Since the currently used internal standards (tetracosane, 2-hydroxycinnamic acid) have non-ideal retention times or response factors that are too large, an internal standard more like the dimers being analyzed was sought. In this study, we used monomethylated 5-5-DFA produced by methylation of diethyl 5-5-diferulate using dimethyl sulfate, followed by column purification on silica gel and saponification. Although it worked well for this study, the standard cannot be recommended at this time for the following reasons. It was not discovered until well into this study that the standard was contaminated by its dimethylated analog, peak IS* in Fig. 2. Subsequent attempts to purify the compound failed. Since response factors were derived for IS against the authentic diferulates, the quantitative aspects of this study are sound, but in future studies it will be necessary to find or prepare a pure internal standard (see previous report — "Diferulates Analysis: Diferulates and Disinapates in Insoluble Cereal Fiber").

Plant Material. Whole grains of corn, wheat, spelt and rice were obtained from a German supplier.

Preparation of insoluble fiber. Samples were milled to a particle size smaller than 0.5 mm. The sample material (10 g) was suspended in phosphate buffer (0.08 M, pH 6.0, 300 mL) and 750 μL of α-amylase were added. The beakers were placed in a boiling water bath for 20 min and shaken gently every 5 min. The pH was adjusted to 7.5, and samples were incubated with 300 μL protease at 60 °C for 30 min with continuous agitation. After adjusting the pH to 4.5, 350 μL amyloglucosidase were added and the mixture was incubated at 60 °C for 30 min with continuous agitation. The suspension was centrifuged, the residue was washed two times with hot water, 95% ethanol and acetone and finally dried at 60 °C overnight in a vacuum oven.

Saponification of insoluble fiber and extraction of ester linked phenolics. Insoluble fiber (40–90 mg) was weighed into a screw-cap tube, internal standard (5–50 μg) dissolved in dioxane was added and saponification with NaOH (2 M, 5 mL) was carried out under nitrogen and protected from light for 18 h at room temperature. Samples were acidified with 0.95 mL concentrated HCl (resulting pH < 2) and extracted into diethyl ether (4 mL, three times). Extracts were combined and evaporated under a stream of N_2. Finally, samples were dried under vacuum.

GC-FID and GC-MS analysis of dehydrodiferulic acids. Dried extracts were silylated by adding 10 μL pyridine and 40 μL BSTFA and heating for 30 min at 60 °C in sealed vials. Trimethylsilylated derivatives of phenolic acids were separated by GLC using a 0.2-mm × 25-m DB-1 capillary column (0.33 μm film thickness) (J&W Scientific) and identified by their electron impact mass data collected on a Hewlett-Packard 5970 mass-selective detector. He (0.54 mL/min) was used as carrier gas. GLC conditions were as follows: initial column temperature, 220 °C, held for 1 min, ramped at 4 °C/min to 248 °C, ramped at 30 °C/min to 300 °C, held 40 min; injector temperature 300 °C, split 1/50. Mass spectra in the electron impact mode were generated at 70 eV. Semiquantitative determination of 4-O-5-DFA was carried out by GLC using the same column and GLC conditions and a flame ionization detector (detector temperature 300 °C). He (0.4 mL/min) was used as carrier gas.

Results and Discussion

Dietary fiber is defined as that part of foodstuff which is not digested by secretions of the human gastrointestinal tract. Although there are other minor sources, plant cell walls constitute the major part of dietary fiber.

In all investigated insoluble cereal fibers the 8-5- and 8-8-coupled diferulic acids as well as the 8-O-4- and 5-5-coupled diferulic acids were identified after saponification by their relative retention times, Fig. 2, and their mass spectra. These diferulic acids have previously been identified in cocksfoot, switchgrass and suspension-cultured corn, sugarbeet, water chestnuts, corn bran, and carrots. Interestingly, the 8-O-4, 8-5- and 8-8-diferulic acids but not the 5-5-diferulic acid were identified in elongating pine hypocotyls. In none of these investigations could the theoretically possible 4-O-5-DFA be identified unambiguously.

In the extracts of saponified corn insoluble fiber 4-O-5-coupled diferulic acid was identified by comparison of its mass spectrum and its relative GLC retention time with that of the genuine compound, which was synthesized and authenticated by NMR. Fig. 1 of the previous report (“Diferulates Analysis: Diferulates and Disinapates in Insoluble Cereal Fiber”) shows the MS spectrum of silylated 4-O-5-DFA (compound **9**); with originally one phenolic and two acid groups, its nominal molecular mass is 602. The relative retention time of 4-O-5-DFA against the internal standard was 1.032. From the insoluble fibers of wheat, spelt and rice the 4-O-5-DFA was identified by its relative GLC retention time, and detection of the molecular peak m/z 602 in selected ion chromatograms.

Semiquantitative determination of 4-O-5-DFA was carried out by setting the response factor as 1.0. Determination of the accurate response factor was not possible because of the tiny amounts of synthesized 4-O-5-DFA available. The response factors of the other diferulic acids, which could be synthesized in larger amounts, against the internal standard were close to 1 (0.91-1.18, with the exception of the 8,5-cyclic-coupled DFA, which is 2.2). The amounts of 4-O-5-DFA in insoluble cereal fibers were 33±3, 13±1, 10±1, and 8±2 μg/g in corn, spelt, wheat, and rice, respectively. Consequently, the amounts of 4-O-5-DFA are approximately 70–100 times lower than the amounts of the sum of 8-5-coupled diferulic acids, which were identified as the major diferulic acids in the cereal fibers investigated. These results therefore provide evidence for the full range of possible ferulate radical coupling products in cereal and presumably in other plant cell walls containing ferulates and diferulates. They also confirm the prevalence for coupling at ferulate’s 8-position (to give the more predominant 8-5-, 8-8-, and 8-O-4 dimers), as also observed in ferulate cross-coupling into lignin .

Conclusions

Alkali-releasable 4-O-5-DFA has been detected in plant materials. The relatively high signal-to-noise chromatograms from the methods described here allow the product to be definitively identified. Its identification as an, albeit minor, diferulate supports its role in the important cell wall cross-linking reactions achieved by ferulate dehydrodimerization. The finding completes the spectrum of ferulate dehydrodimers to be found in plants, and supports the concept of free-radical coupling of cell wall components independently of enzymes or proteins which might otherwise confer a strict regiochemical course, i.e. produce only a single diferulate.

The complete manuscript is available from our website at:
http://www.dfrc.ars.usda.gov/DFRCWebPDFs/2000-Bunzel-JAFC-48-3166.pdf

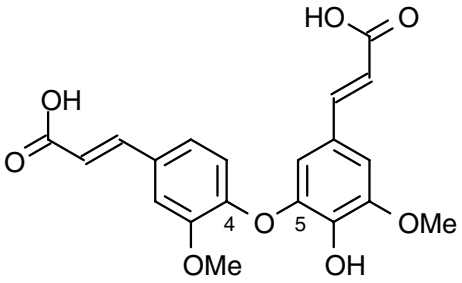

Fig. 1. Structure of 4-O-5-coupled diferulic acid.

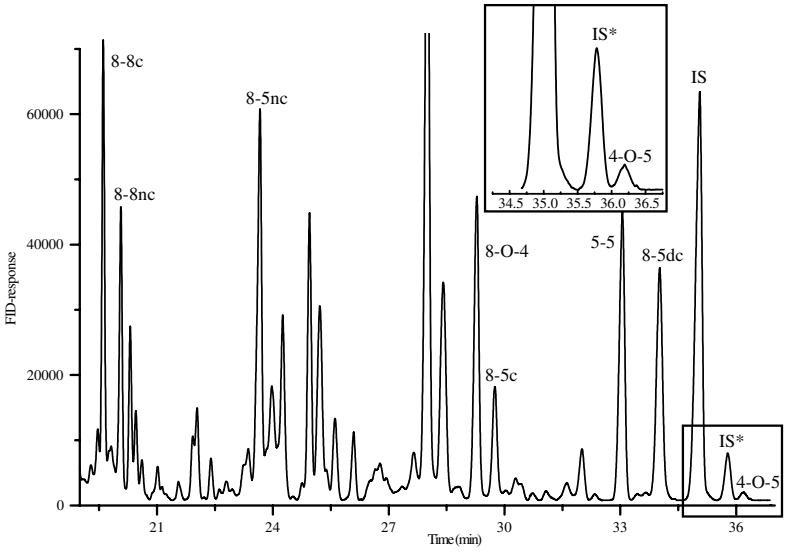

Fig. 2. GC-FID chromatogram of the extract of saponified spelt insoluble fiber.
8-8-coupled diferulic acids: c – cyclic, nc – non cyclic; 8-5-coupled diferulic acids: nc – non cyclic, c – cyclic, dc – decarboxylated. Many of the unlabelled peaks have been assigned as ferulate cross-products, as will be detailed elsewhere.

5-Hydroxyconiferyl Alcohol as a Monolignol in COMT-deficient Angiosperms

J.M. Marita, F. Lu, J. Ralph, R.D. Hatfield, C. Lapierre, S.A. Ralph, C. Chapple, W. Vermerris, W. Boerjan, and L. Jouanin.

Introduction

Recent advances in genetic engineering have allowed researchers to perturb the monolignol biosynthetic pathway producing often significantly altered lignins. This approach provides valuable insights into the control of lignification and into the apparent biochemical flexibility of the lignification system.

Here we present NMR and DFRC data from recent studies on mutants and transgenics deficient in COMT (caffeic acid *O*-methyl transferase), the favored substrate for which now appears to be 5-hydroxyconiferyl aldehyde. Downregulating these enzymes dramatically affects the composition of lignins and the structures contained in those lignins.

COMT-Deficient Poplar: Benzodioxanes from Incorporation of 5-Hydroxyconiferyl Alcohol.

COMT is one of two enzymes required to 5-methoxylate guaiacyl monomeric units to produce sinapyl alcohol and eventually produce syringyl units in angiosperm lignins. If COMT is downregulated, 5-hydroxyconiferyl aldehyde might be expected to be reduced to 5-hydroxyconiferyl alcohol if the next reductase enzyme is sufficiently non-specific. In fact, it appears that 5-hydroxyconiferyl alcohol is indeed formed, shipped out to the wall, and incorporated into lignin analogously to other lignin monomers (although it produces some novel structures in the final lignin), Fig. 1.

NMR provides beautiful evidence that benzodioxane structures are produced in lignins which incorporate 5-hydroxyconiferyl alcohol. Figure 2b shows the sidechain region of an HMQC spectrum from an (acetylated) isolated lignin from a COMT-deficient poplar (*Populus tremula* x *Populus alba)* described recently. The benzodioxanes **H** are readily apparent. Well separated contours at δ_C/δ_H of 76.8/4.98 (α), and 75.9/4.39 (β) are diagnostic for the benzodioxanes **H**; the γ-correlations overlap with those in other lignin units, but are elegantly revealed in 3D TOCSY-HSQC (see accompanying Report—"The first 3D NMR of un-enriched lignin. Proof of benzodioxanes in a COMT-deficient angiosperm") or 2D-HMQC-TOCSY spectra. The sidechain correlations are consistent with those in a model compound for the *trans*-benzodioxane, synthesized by biomimetic cross-coupling reactions between coniferyl alcohol and a 5-hydroxyguaiacyl unit.

A reasonable quantification of this unit can be achieved by measuring volume integrals in the 2D spectra, particularly if the similar Cα–Hα correlations are used. The ratios in the transgenic poplar (and in the wild-type control) are given in Table 1. The 5-hydroxyconiferyl alcohol-derived benzodioxane **H** units are the second most abundant (~18%) interunit type in the COMT-gene-silenced sample. Since the lignins analyzed by NMR represent 65% of the total lignin in this transgenic, it is logical that the benzodioxane structures would remain a significant component even if the lignins were drastically partitioned by the isolation process. The total β-ether frequency (normalβ-ether**A** plus dibenzodioxocins **D** plus benzodioxanes **H**) in the transgenic is around 78%, lower than in the control because of the higher guaiacyl content. However, there are a few units not covered by these percentages since they have no resonances in the aliphatic sidechain region of the NMR spectra (cinnamaldehyde endgroups, β–1-structures). Lignins from COMT antisense poplars

also contain benzodioxane units at a lower level. Although the data are limited at present, it appears that 5-hydroxyconiferyl alcohol may largely make up for the sinapyl alcohol deficiency.

Evidence for 5-hydroxyconiferyl alcohol incorporation and of benzodioxane units in the lignins also comes from degradative analyses (see the accompanying report — "Marker Compounds for Enzyme Deficiencies in the Lignin Biosynthetic Pathway. 2. COMT"). What the degradative and NMR data show is that 5-hydroxyconiferyl alcohol is behaving like a normal monolignol does in lignification. It reacts at its β-position with the phenol at the end of the growing lignin polymer, and new monolignols then react with the resulting new 5-hydroxyguaiacyl phenolic end. This endwise polymerization is characteristic of the major lignification pathway. It also indicates that 5-hydroxyconiferyl alcohol appears to be incorporating intimately into the polymer in the same way that the traditional monolignols do. We see no reason therefore why 5-hydroxconiferyl alcohol should not be considered an authentic monolignol in these systems.

Benzodioxanes in F5H-Upregulated Arabidopsis.

There is another interesting variant in the COMT-deficiency class. Arabidopsis transgenics with upregulated F5H have previously been shown to have only a minor guaiacyl component. Contours previously unidentified in the 2D NMR spectra of their lignins now obviously result from benzodioxane structures, Fig. 2c. The observations here imply that, whereas syringyl production was enormously up-regulated in these transgenics, the methylation could apparently not keep pace with the accelerated production of 5-hydroxy-units (e.g. 5-hydroxyconiferyl aldehyde and 5-hydroxyconiferyl alcohol). The result is a significant incorporation of 5-hydroxyconiferyl alcohol into the monolignol pool for the most heavily F5H-upregulated transgenics, ~10% as measured from contour volumes in the HMQC spectra — see Table 1.

Benzodioxanes in *bm3* Maize Mutants

Maize has four brown-midrib (*bm*) mutants, all of which have reddish-brown vascular tissue in the leaves and stems. Two are known to have mutations in the monolignol biosynthetic pathway; *bm1*, CAD; *bm3*, COMT.

Lignins in the *bm3* mutant show the now characteristic signs of 5-hydroxyconiferyl alcohol incorporation. Early on, thioacidolysis suggested that 5-hydroxyconiferyl alcohol was a constitutive unit of those lignins. The dimeric benzodioxane products from thioacidolysis and DFRC are also readily identified in the maize mutant. Preliminary NMR of isolated lignins shows the substantial presence of these new **H** units in the mutant (Table 1) where it accounts for some 25% of the interunit linkages characterized (although we have not yet examined how this structure is partitioned between the soluble fraction used for NMR and the residues).

Implications for Pulping

How is offsetting syringyl units in lignins with 5-hydroxyguaiacyl units likely to affect pulping performance? The new benzodioxane units in the lignin are still ether structures (a,b-diethers), but will they cleave under pulping conditions? In preliminary studies with etherified benzodioxane model compounds, very little ether cleavage occurs under soda pulping conditions— the models are recovered intact in high yields. Kraft pulping conditions are unlikely to affect the outcome. With less

cleavable b-ethers in the lignin, pulping efficiency would therefore likely be reduced. Recent pulping trials with COMT-deficient poplars confirm a lower pulping efficiency (Jouanin et al., 2000). In part this may also be attributed to the slightly higher guaiacyl content in the transgenic lignins compared with the wild-type control, but it is suspected that much of the effect can be attributed to the alkaline stability of the benzodioxanes.

Implications for Ruminant Digestibility

No clear correlations between lignin structure and cell wall digestibility in ruminants are evident. However, various mutants and transgenics are of interest because of their potential to improve digestibility. At present, such studies remain empirical. Dixon's group at the Noble Foundation are examining digestibility implications of various alfalfa transgenics, including those deficient in COMT, and we are currently structurally analyzing their plants.

Conclusions

As further evidence accumulates from degradative and NMR methods that 5-hydroxyconiferyl alcohol monomers integrate into the polymerization process, it becomes evident that 5-hydroxyconiferyl alcohol can be used as a lignin monomer by plants, in part offsetting the deficiency in sinapyl alcohol monomers. A salient observation is that the process of lignification appears to be flexible enough to incorporate phenolic phenylpropanoids other than the traditional monolignols. The incorporation of 5-hydroxyconiferyl alcohol (as well as hydroxycinnamyl aldehyde monomers in CAD-deficient angiosperms) also implies that the plant is sending these products of incomplete monolignol biosynthesis out to the cell wall for incorporation. The resultant modified lignins apparently have properties sufficient to accommodate the water transport and mechanical strengthening roles of lignin and to allow the plant to be viable. Whether such plants will be able to confront the rigors of a natural environment replete with a variety of pathogens remains to be determined. However, the plants' approach toward lignification, i.e. polymerizing monolignol precursors and derivatives along with the traditional monolignols, is a testament to a flexible survival strategy; in a single generation, these plants have circumvented genetic obstacles to remain viable. The recognition that monolignol intermediates and other novel units can incorporate into lignin provides expanded opportunities for engineering the composition and consequent properties of lignin for improved utilization of valuable plant resources.

Fig. 1. Production of benzodioxanes **7** in lignins via incorporation of 5-hydroxyconiferyl alcohol **1** into a guaiacyl lignin. Only the pathways producing β-ether units are shown. Cross-coupling with syringyl units is less pronounced in lignins which have a low syringyl content due to COMT downregulation. Cross-coupling of 5-hydroxyconiferyl alcohol **1**, via its radical **1·**, with a guaiacyl lignin unit **3G**, via its radical **3G·**, produces a quinone methide intermediate **4** which re-aromatizes by water addition to give the β-ether structure **5** (possessing a 5-hydroxyguaiacyl end-unit). This unit is capable of further incorporation into the lignin polymer via radical coupling reactions of radical **5·**. Reaction with the monolignol coniferyl alcohol **2G**, via its radical **2G·**, produces a quinone methide intermediate **6**. This time, however, quinone methide **6** can be internally trapped by the 5-OH phenol, forming a new 5–O–α-bond, and creating the benzodioxane ring system in **7**. The presence of structures **7** in COMT-deficient transgenic plants is diagnostically revealed by NMR, units **H** in Fig. 2.

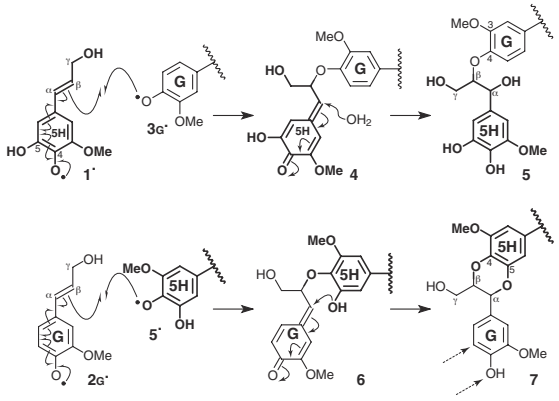

Fig. 2. Partial spectra from gradient HMQC NMR experiments highlighting new peaks for benzodioxane units **H**. Lignins were from a) a control poplar, b) a COMT-downregulated transgenic, c) an F5H-upregulated Arabidopsis, and d) similar correlations from a benzodioxane model.

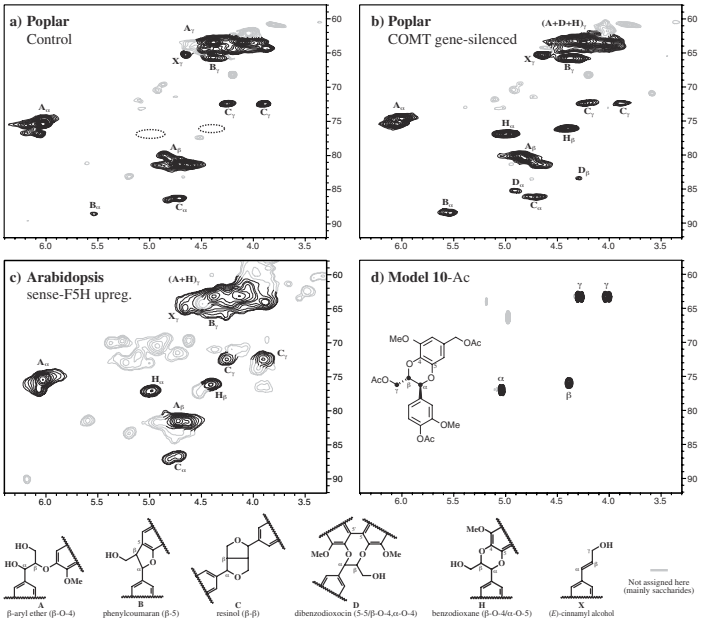

Table 1. Subunit ratios derived from volume integrals of contours in the sidechain region of ^{13}C–^{1}H correlation spectra of acetylated isolated lignins.

Lignin	A	B	C	D	H	X	β-O-4
Poplar							
WT	88	3	7	0	0	2	88
COMT-silenced	53	13	5	6	18	5	78
COMT-anti	65	12	5	3	10	4	78
Maize							
WT	86	7	0	0	0	6	86
bm3-mutant	60	7	0	0	25	8	85
Arabidopsis							
WT	67	13	6	6	0	7	73
F5H-sense	81	<1	6	0	10	4	91

A = β-ether (β-O-4), **B** = phenylcoumaran (β-5), **C** = resinol (β-β), **D** = dibenzodioxocin (β-O-4/α-O-4), **H** = benzodioxane (β-O-4/α-O-5); the last column is the sum of all β-O-4 components (**A**+**D**+**H**). Note: these values are simple area ratios of these 6 units, and should not be interpreted as percentages of interunit linkages in lignin, since 5–5, β–1, and other linkages are not included.

Marker Compounds for Enzyme Deficiencies in the Lignin Biosynthetic Pathway. 1. CAD

H. Kim, J. Ralph, F. Lu, I. Mila, B. Pollet, and C. Lapierre.

Introduction

Perturbations of the lignin biosynthetic pathway have the potential to enhance the utilization of plant cell walls in various natural and industrial processes. In forages fed to ruminant animals, lignins inhibit the rumen-degradability of polysaccharides. In chemical pulping for paper production, the aim is to selectively remove the lignin from the cellulose fibers. Recently it has become evident that there is potential beyond simply down-regulating lignification itself to produce low-lignin plants. Inducing structural and compositional changes in the polymer may also be beneficial for many processes.

The definitive way to determine a plant's response to up- or down-regulation of lignin-biosynthetic-pathway genes/enzymes and the impact on the lignification process itself is by lignin structural analysis. However, full structural analysis is a lengthy and difficult process inappropriate for screening. Marker compounds that allow the degree of change to be elucidated are vital particularly when various levels of down-regulation need to be assessed.

CAD (cinnamyl alcohol dehydrogenase) is the last enzyme on the pathway to the monolignols, primarily coniferyl and sinapyl alcohols, from which polymeric lignin is derived. CAD deficiency in various mutant and transgenic plants has been reported to induce the increased incorporation of hydroxycinnamyl aldehydes into the lignin polymer. Recent NMR studies revealed that, in a CAD-deficient tobacco, sinapyl aldehyde readily 8–O–4-coupled with both syringyl (S) and guaiacyl (G) lignin units, and that coniferyl aldehyde also 8–O–4-cross-coupled but only with S-units.

Radical coupling of an hydroxycinnamyl aldehyde at its 8-position results initially in a quinone methide. Unlike in the β–O–4-coupling of hydroxycinnamyl alcohols, where re-aromatization is by nucleophilic addition of water to the quinone methide, the hydroxycinnamyl aldehyde quinone methide 8–O–4-coupling product re-aromatizes by elimination of the acidic 8-proton to give the unsaturated 8–O–4-product **3**, Fig. 1; this elimination was observed in the dimerization reactions of coniferyl aldehyde and has recently been established for both coniferyl and sinapyl aldehydes in lignification as well.

Hydroxycinnamyl aldehydes either involved in 8–O–4-linkages or incorporated as 4-O-β-end-groups **6**, Fig. 1, will release diagnostic monomers following thioacidolysis, which therefore serve as marker compounds for hydroxycinnamyl aldehyde incorporation. Consequently, they also serve as maker compounds for CAD-deficiency. This paper details the identification of thioacidolysis CAD marker compounds, and provides evidence that 8–O–4-coupled hydroxycinnamyl aldehyde units in lignin are their source.

Results and Discussion

Two new isomeric monomers have been systematically detected following thioacidolysis of a range of CAD-deficient dicots in the INRA laboratories. The compound levels appeared to vary with the amount of CAD-downregulation (see Fig. 55 later). These isomers had a nominal MW of 312 and an apparent formula $C_{15}H_{20}O_3S_2$. Raney nickel desulfurization generated a single new monomer (nominal MW 194, $C_{11}H_{14}O_3$). The latter was found by GC-MS to be not the commercially available

syringyl prop-1-ene **7** (Fig. 2), nor the pro-2-en **8** that could be prepared by Rh(III)-assisted isomerization, both of which had different GC retention times. Syringyl cyclopropane **9** appeared to be a possibility particularly since DFRC-degradation of cinnamyl aldehydes produced cyclopropanes. However, synthesized **9** also had a GC retention time which differed from the thioacidolysis-Raney-Ni product. The only possibility left (while retaining the syringyl moiety) was the indane **10**. However, its authentication was required and the exact structures of the precursor thiol products also remained unresolved. Rather than synthesize suspected compounds independently, we sought to elucidate the source of the thioacidolysis products using model compounds, and to prepare sufficient products for isolation and full structural characterization, along with establishing their identity to the thioacidolysis products.

Since thioacidolysis rather specifically cleaves ether linkages, the only likely source of the compounds was β-ether units **6** or **3**, Fig 1. However, we already know that products R–CHSEt–CH_2–$CH(SEt)_2$ result from coniferyl and sinapyl aldehydes and from their ethers **6**. The likely source of the new compounds was therefore logically from 8-O-4-coupled hydroxycinnamyl aldehyde units **3**.

Model compounds for hydroxycinnamyl aldehyde 8–O–4-units **3** were synthesized. Thioacidolysis of the model compound for **3SG** did indeed cleanly give the same two isomeric compounds as thioacidolysis of CAD-deficient plants, in approximately equal amounts, Figure 3. With similar mass spectra, the structures could only be reliably elucidated by NMR. The isomers were separated by preparative TLC or HPLC.

Proton NMR showed that one of the isomers (the faster moving isomer) had two aromatic or double-bond protons and one aliphatic proton (presumably with a thioethyl group on the same carbon), whereas the slower isomer had only one aromatic and two aliphatic protons. Full structural elucidation by the usual complement of 1D and 2D NMR methods revealed them to be isomers **11S** and **12S** related by a 1,3-sigmatropic proton shift by which they presumably equilibrate under the thioacidolysis conditions. These structures are logical from the anticipated thioacidolysis mechanisms, Figure 4, at least in hindsight. Raney nickel desulfurization of either (or a mixture) of the two isomers **11S/12S** gave the indane **10S** reasonably cleanly. Only one guaiacyl analog of compound **12S** could be observed, together with the product G–CHSEt–CH_2–$CH(SEt)_2$ derived from coniferyl aldehyde end-groups. This result suggests that down-regulating CAD activity in poplar specifically affects the reduction of sinapyl aldehyde into sinapyl alcohol.

The importance of the new markers (**11S + 12S**), relative to the conventional syringyl monomers (S–CHSEt–CHSEt–CH_2SEt), was found to increase together with the level of CAD deficiency (Fig. 5). This signature was observed even before any wood phenotype (red coloration of the xylem) could be seen or before any other lignin structural alteration could be detected.

Conclusions

Marker compounds (released following the application of degradative methods) for CAD-deficiency have been identified and their sources in the novel lignins elucidated. The thioacidolysis CAD-markers come from hydroxycinnamyl aldehyde units linked 8–O–4 to generic lignin units. Such marker compounds become valuable in assessing the effects of various levels of down-regulation in CAD-deficient plants.

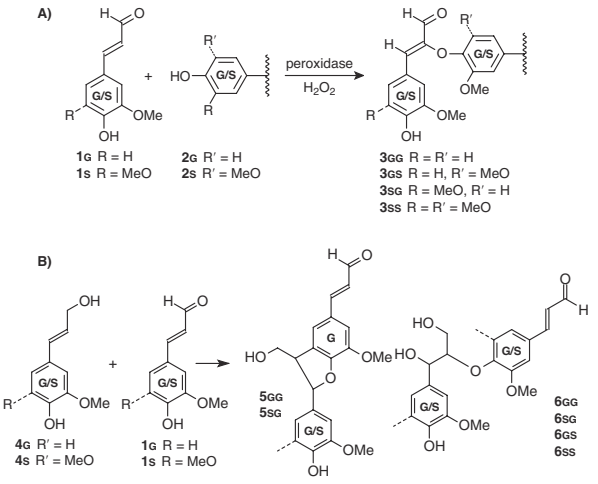

Fig. 1. Possible modes of incorporation of hydroxycinnamyl aldehydes **1** into the lignins of CAD-deficient plants. A) The four products possible from 8–O–4-cross-coupling with lignin S and G units **2**. **3GG** is not observed in vitro or in vivo (in tobacco). B) Possible products from coupling at the aromatic sites (4-O- or 5-), resulting in hydroxycinnamyl aldehyde end-units (**5** or **6**) in lignins.

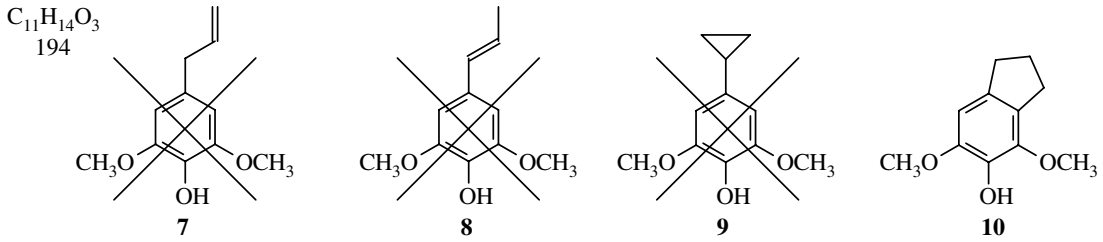

Fig. 2. Possible structures for the MW 194 marker compounds from thioacidolysis followed by Raney-Ni desulfurization.

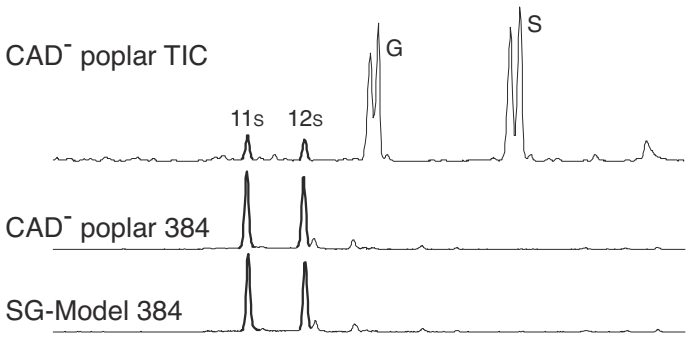

Fig. 3. GC-MS traces showing the two thioacidolysis CAD markers in the transgenic poplar (total ion chromatogram and selected-ion chromatogram (m/z 384, silylated) and the analogous selected-ion chromatogram from thioacidolysis of the 8–O–4-model compound for **3SG**.

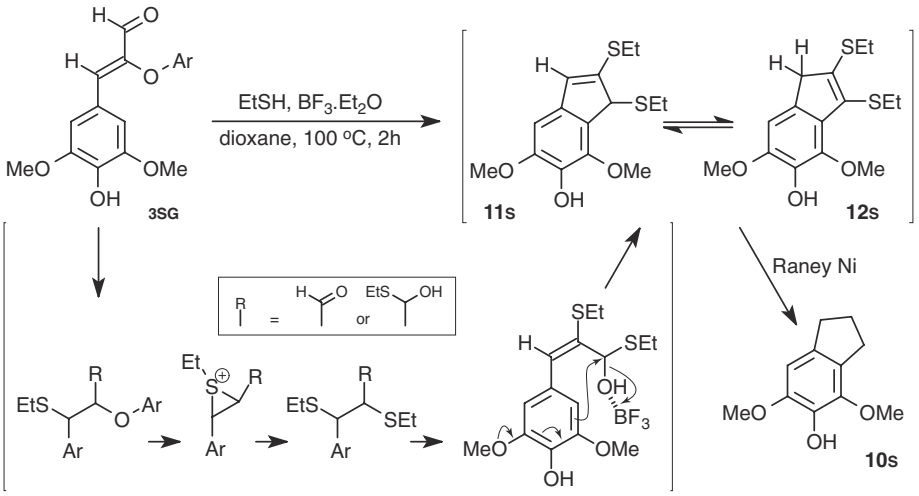

Fig. 4. Thioacidolysis of the model compound for **3SG** or of similar units in the lignin.

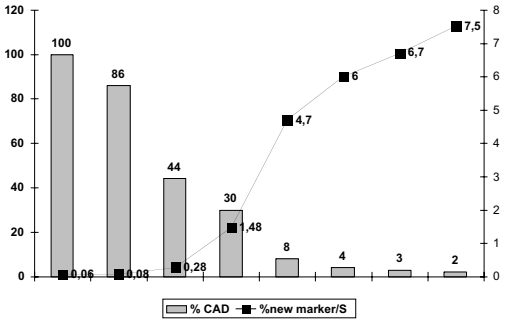

Fig. 5. Relative importance of the thioacidolysis markers of CAD deficiency in poplars, [%(**11S** + **12S**)/Conventional S], as a function of residual CAD activity level (100% = control level). Sample with 44% residual activity does not show any red xylem phenotype. Sample with 30% residual activity correspond to the ASCAD21 line displaying a red phenotype. Samples with activity <10% are OGY70ASCAD different lines. Data from Lapierre, INRA, France.

Marker Compounds for Enzyme Deficiencies in the Lignin Biosynthetic Pathway. 2. COMT

F. Lu, J.M. Marita, J. Ralph, I. Mila, B. Pollet, and C. Lapierre.

Introduction

As described more fully in the introduction to Part 1, the preceding article, marker compounds that are diagnostic for a given gene downregulation and allow the degree of change to be elucidated are vital particularly when various levels of down-regulation need to be assessed.

COMT is the final methylating enzyme in the production of sinapyl alcohol monolignols. Its down-regulation results in a build-up of 5-hydroxyconiferyl alcohol which is exported to the wall and intimately incorporated into lignins forming novel benzodioxane structures in the polymer, as shown in Fig. 1 of a preceding Report "5-Hydroxyconiferyl alcohol as a monolignol in COMT-deficient angiosperms". Thioacidolysis, and also our DFRC method, produce diagnostic marker compounds from these novel lignin units.

Results and Discussion

Thioacidolysis of COMT-deficient brown-midrib mutants had earlier suggested that 5-hydroxyconiferyl alcohol was a constitutive unit of those lignins. A monomeric compound **1** was released, Fig. 1. More recently, a dimeric benzodioxane compound **2** was also observed following Raney-Ni desulfurization of thioacidolysis products from COMT-deficient poplar transgenics. The DFRC degradative method also produced diagnostic benzodioxane dimers **3**, but no monomeric 5-hydroxyguaiacyl products. Model studies showed that the DFRC method leaves benzodioxanes completely intact, whereas thioacidolysis partially cleaves them (into monomeric products). The absence of monomeric 5-hydroxyguaiaicyl DFRC products strongly suggests that all such units in the lignins are present in benzodioxane structures. GC(-MS) data for the DFRC products are shown in Fig. 2.

These benzodioxane marker compounds are not released in great amounts, but are nevertheless diagnostic and their detection is sensitive enough that they are likely to become useful measures of COMT-downregulation.

Mechanistic Implications

The release of compounds **3G** and **3S** following DFRC degradation are more diagnostic than might at first be assumed. The following observations are relevant.

1. The double bond implies that the 5-hydroxyconiferyl alcohol unit had coupled β-O-4 to a syringyl or guaiacyl unit in lignin. It could not have been another 5-hydroxyguaiacyl unit or dimer **3** would not be released. In fact, it also is not likely to have been incorporated by reaction with another monolignol, since cross-coupling studies are showing that it is coniferyl or sinapyl alcohol that couples at the β-position and the 5-hydroxyconiferyl alcohol couples at the 4-O-position. This is borne out in the literature by the isolation of several lignans similar to **3** but none have been reported with reverse coupling modes (i.e. coupling at the β-position on the 5-hydroxyconiferyl alcohol unit).

2. Since we can readily identify both compounds **3S** and **3G**, we obviously know that monolignols, sinapyl or coniferyl alcohol, then react at their β-positions with the newly formed hydroxyguaiacyl unit (at its 4-O-position) on the growing polymer.
3. The NMR data already indicates that the phenol on the guaiacyl unit attached to the benzodioxane in the lignin is etherified. Since DFRC releases units **3**, there must also be further etherification presumably by another monolignol (at its β-position)– again, it could not be another 5-hydroxyconiferyl alcohol or it would not release dimer **3**. Further DFRC experiments will be able to establish what proportion of these released benzodioxanes were originally etherified.

Conclusions

Marker compounds (released following the application of degradative methods) for both COMT-deficiency have been identified and their sources in the novel lignins elucidated. Thioacidolysis monomeric and dimeric, and DFRC dimeric COMT markers originate from benzodioxane structures in the lignins which themselves result from the incorporation of 5-hydroxyconiferyl alcohol monomers. Most importantly they establish that the novel 5-hydroxyconiferyl alcohol monomer is coupling with normal lignin units, and that coniferyl alcohol will then couple with the new 5-hydroxyguaicyl end unit that is formed. As such, the novel monomer appears to be incorporating intimately into the lignin. The thioacidolysis and DFRC marker compounds become valuable in assessing the effects of various levels of down-regulation in COMT-deficient plants.

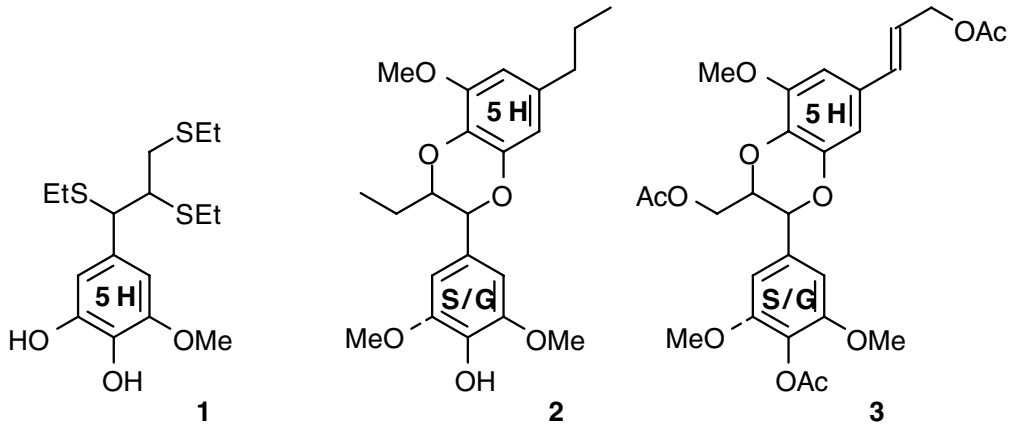

Fig. 1. Marker compounds for 5-hydroxyconiferyl alcohol incorporation into lignins (and COMT deficiency); thioacidolysis monomeric marker **1**, dimer **2** (following Raney-Ni desulfurization), and DFRC marker **3**.

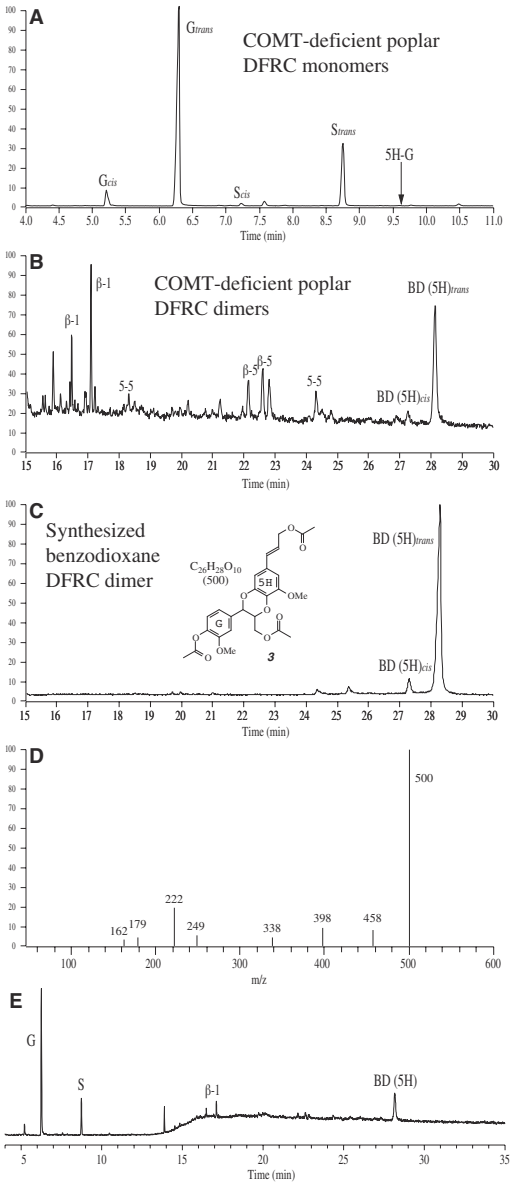

Fig. 2. DFRC Benzodioxane Markers for COMT-deficiency. A. DFRC monomer region of COMT deficient poplar showing no 5-hydroxyguaiacyl monomers — thioacidolysis monomers contain the diagnostic 1,2,3-trithioethylguaiacylpropane. B. The DFRC dimers region showing the benzodioxane components. C. The synthesized DFRC benzodioxane product for authentication. D. MS of the guaiacyl benzodioxane. E. Low-res GC-MS TIC of entire chromatogram (monomer and dimer regions) showing that the benzodioxane in this gene-silenced poplar lignin is released in easily detectable amounts.

The First 3D NMR of Un-enriched Lignin. Proof of Benzodioxanes in a COMT-deficient Angiosperm

J. Ralph and J.M. Marita

Introduction

NMR spectroscopy is an exceptionally powerful tool for determining organic structures, even in a polymer as complex and heterogeneous as lignin. We have recently reviewed the application of 2D NMR to lignin, providing a multitude of colored figures to aid interpretation - this article is also available from our web site: http://www.dfrc.ars.usda.gov/DFRCWebPDFs/1999-Ralph-TAPPI-55.pdf.

Three–dimensional (and/or higher-dimensional) NMR experiments are routinely applied to labeled proteins. Some success has come from applying the 3D HMQC-TOCSY (with one ^{13}C and two ^{1}H axes) to synthetic lignins, and to uniformly ^{13}C-enriched lignins, but the literature suggests that such experiments are difficult with real isolated unlabeled lignins. Here we report not only the first 3D NMR of an isolated lignin that has not been ^{13}C-enriched, but one which firmly establishes the presence of benzodioxane units in a COMT transgenic, as described further in an accompanying Report ("5-Hydroxyconiferyl alcohol as a monolignol in COMT-deficient angiosperms"). The "isolation" of the novel structural unit by 3D NMR is, in our humble opinion, spectacular.

Experimental

The 2D (two-dimensional) NMR spectra were taken on our Bruker DRX-360 instrument fitted with a 5-mm ^{1}H/broadband gradient probe with inverse geometry (proton coils closest to the sample). The conditions for all samples were ~100 mg of acetylated lignin in 0.4 ml of acetone-d_6, with the central solvent peak as internal reference (δ_H 2.04, δ_C 29.80). The standard Bruker implementations of gradient-selected versions of inverse (^{1}H-detected) heteronuclear multiple quantum coherence (HMQC) experiments were used. The 3D (three-dimensional) NMR experiment was acquired on a Bruker DMX-750 instrument fitted with a 5-mm triple-resonance (^{1}H, ^{13}C, ^{15}N) gradient inverse probe. The 3D gradient-selected TOCSY-HSQC experiment was trivially modified to a two-channel version from "mlevietf3gs3d" (a 3 channel experiment). The TOCSY spin lock period was 70 ms in this case; 2D TOCSY experiments indicated that, whereas 125 ms was optimal, 70 ms also provided suitable TOCSY transfer especially for new benzodioxane structures. Carbon/proton designations are based on conventional lignin numbering. Lignin sub-structures are labeled by the convention established in a recent book chapter (Advances in Lignocellulosics Characterization).

Results and Discussion

Figure 1 shows the first 3D gradient-selected TOCSY-HSQC spectrum of a natural ^{13}C-abundance lignin. It is the acetylated lignin from the sense-suppressed COMT transgenic taken on a high magnetic field 750 MHz instrument. In less than 24 hours, the 3D experiment provided ample sensitivity to authenticate all of the major units in the natural ^{13}C-abundance sense-suppressed COMT transgenic lignin. Analogous experiments run on a 360 MHz instrument over 60 h were similarly successful.

In the 3D TOCSY-HSQC experiment, spectra are acquired with three orthogonal dimensions, labeled F_1, F_2, and F_3. The acquired dimension is F_3 (proton). F_2 is carbon and F_1 is proton. A slice in the F_2-F_3 plane is basically a 2D ^{13}C-^{1}H HSQC spectrum at a given proton chemical shift (defined by the position along the proton F_1 axis). 2D F_2-F_3 projections/slices for the prominent structures in the lignin are shown in Figs 1d-g. The slices show: a) the 3D contour map; b) a 2D HMQC for comparison with; c) the first 2D slice in the F_2-F_3 plane (which is essentially a 2D composite spectrum of all the units on all the other planes); d-g) F_2-F_3 slices at various proton frequencies (in F_1) showing almost perfect isolation of the major structural units in HSQC-type sub-spectra.

When a proton frequency is unique to a given structure, a "pure" F_2-F_3 slice and HSQC of only that structure can be obtained. F_2-F_3 slices for both the β-aryl ether **A** units and phenylcoumaran **B** units at their respective α-proton frequency along the proton F_1 axis show this phenomenon nicely, Figs 1d,e. Only ^{13}C-^{1}H correlations for the given unit are seen in each slice. Fig. 1d is a "pure" slice of β-aryl ether **A** units at the α-proton frequency of 6.05 ppm. This slice shows both *syn*- and *anti*-β-ether isomers. Slices either side of this slice (not shown) resolve *syn*- from *anti*-isomers. Fig. 1e is a "pure" slice of phenylcoumaran **B** units at the α-proton frequency of 5.62 ppm. However, a "pure" F_2-F_3 slice of the resinol **C** units is not obtainable at any of its proton frequencies. The best slice represents resinol **C** units at its β-proton frequency of 3.09 ppm, Fig. 1f. At this particular frequency some saccharides/methoxyl peaks are also detected but the slice uniquely isolates all of the resinol **C** units. The F_2-F_3 slice of the new benzodioxane structure is spectacular with its α-, β-, and γ-correlations fully resolved, Fig. 1g. In the 3D experiment, the γ-correlations of benzodioxane in the F_2-F_3 plane are nicely resolved and isolated from the plane at its α-proton frequency (5.01 ppm) as well as at the β-proton frequency (~4.47 ppm; not shown) along the F_1 axis. By obtaining a "pure" slice, there is no ambiguity between correlations of different structures. For example, the γ_1- and γ_2-correlations of the benzodioxane units that are unresolved from the γ_1- and γ_2-correlations of the β-aryl ether **A** units and the dibenzodioxocin **D** units in 2D spectra are unique to their respective 3D slices. This is the first reported identification of a new lignin component using 3D NMR experiments at natural abundance. The data in this slice agree with those from a benzodioxane model compound.

Another detail regarding benzodioxane units **H**, the degree of etherification, is revealed in the 3D spectra (and 2D — see Fig. 2 in the accompanying Report, "5-Hydroxyconiferyl alcohol as a monolignol in COMT-deficient angiosperms"). Unfortunately, the ball-milling step in the lignin isolation process produces extra phenolic groups, so isolated lignins have a higher phenolic content than natural lignins. In acetylated lignins, units that were free-phenolic in lignin become phenol-acetylated, whereas those that were originally etherified remain so. Phenol acetylation causes H_α in **H** units to move to a lower field (higher ppm). Thus, unetherified units have H_α at 5.04 ppm, whereas etherified units are at 4.96 ppm. The 2D slice for the 3D experiment shown in Fig. 1g has only a trace of correlations for the acetylated component. Other slices reveal slightly more. However, it appears that the benzodioxane units **H** are substantially etherified and therefore have been fully integrated into the polymer by further monolignol coupling reactions during lignification. Monomer substitution (5-hydroxyconiferyl alcohol for sinapyl alcohol) therefore appears to have been successfully accommodated in these transgenics. The substitution of L-fucose with L-galactose in fucose-deficient *mur1* mutants of Arabidopsis is a previously documented monomer substitution occurring in polysaccharides (Science 272: 1808), where the polymer biosynthesis is more highly structurally controlled than in lignification.

Conclusions

The presence of these novel benzodioxane units in an isolated lignin from a COMT-deficient angiosperm is diagnostically revealed by a 3D NMR experiment. The experiment is able to completely isolate the complete carbon-proton sidechain network onto its own 2D plane, authenticating the structure and establishing the elusive gamma-correlations. From the plant point of view, the finding indicates that the plant is capable of sending the intermediate monolignol 5-hydroxyconiferyl alcohol out into the cell wall for incorporation. The realization that novel units such as benzodioxanes can be tolerated in lignins should encourage further research into bioengineering plants with broad compositional changes in their lignins in order to achieve enhanced cell wall digestibility and/or reduction of negative environmental impacts of chemical pulping and bleaching related to papermakin

Fig. 1. 3D NMR (750 MHz) "isolation" of the major units in COMT-deficient transgenic poplar lignins. (a) A 3D gradient-selected TOCSY-HSQC spectrum (70 ms TOCSY mixing time) of a natural ^{13}C-abundance lignin (acetylated) from the sense-suppressed COMT transgenic; (b) 2D gradient-selected HMQC spectrum; (c) the first F_2-F_3 plane which is essentially a 2D ^{13}C-^{1}H HSQC spectrum; (d-g) 2D F_2-F_3 slices for the major structural units (**A**, **B**, **C**, and novel **H**). Note: this Figure is made to be viewed in color; please see the web version of these Research Summaries on our web site, or see the original paper containing these spectra: http://www.dfrc.ars.usda.gov/DFRCWebPDFs/2001-Marita-JCSPerkin-2939.pdf

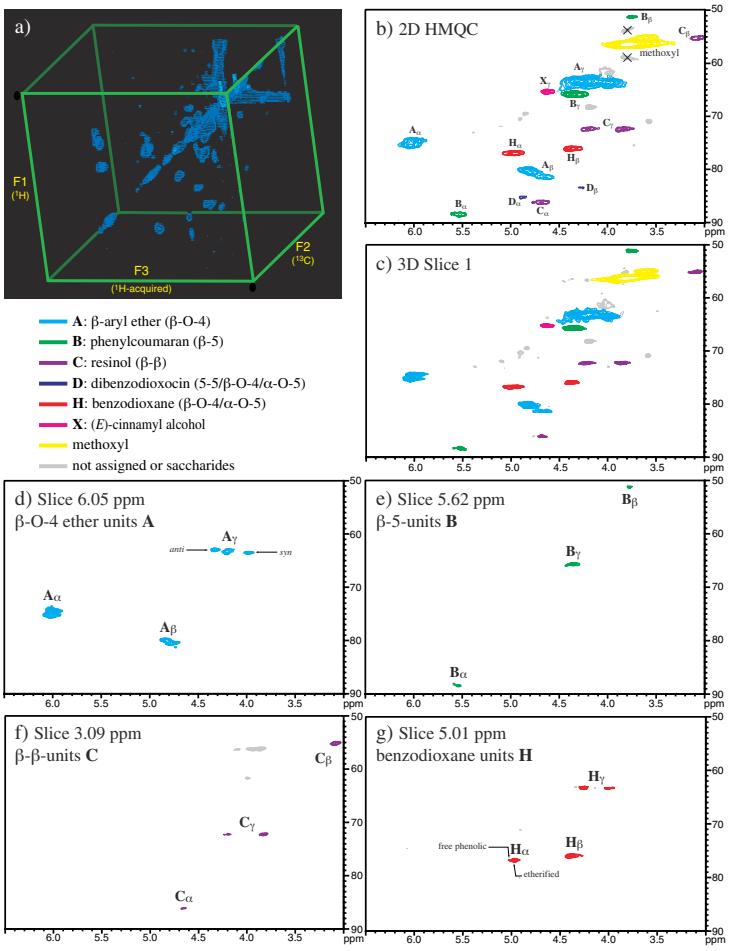

Preliminary Evidence for Sinapyl Acetate as a Lignin Monomer in Kenaf

F. Lu and J. Ralph

Introduction

What does kenaf have to do with forages? Lignins of many agriculturally important crops and woody plants are acylated by various acids, although the biochemistry associated with such acylation remains unresolved and the genes are unknown. Nor is it known if lignin monomers (the hydroxycinnamyl alcohol monolignols) are first acylated to produce ester conjugates which are then incorporated by coupling and cross-coupling into lignin by the traditional free-radical coupling reactions, or whether acylation occurs *following* the monolignol radical coupling reactions or on the lignin polymer itself. These issues are becoming important to resolve as genes controlling the various processes and the functions of such acylation are sought in order to improve the utilization of plant resources, by ruminant animals for example. Acylated components have also been found to increase (on a lignin basis) when lignification is decreased by down-regulating enzymes in the monolignol biosynthetic pathway. Once we understand what the plant is trying to achieve with this lignin acylation, it might be possible to introduce additional drought-tolerance into forages, for example, as well as possibly impact the cell wall digestibility.

NMR of isolated kenaf bast fiber lignins suggested well over 50% lignin acetylation, almost entirely of the sidechains' primary aliphatic alcohols. Our "Derivatization Followed by Reductive Cleavage" ("DFRC") method, which cleaves ether linkages in lignins and releases analyzable monomers and dimers, leaves such esters intact. A modification (termed DFRC′), using propionyl analogs of the normal acetyl reagents, allowed us to establish that the native lignin was about 60% 9-acetylated and, more revealingly, that syringyl (3,5-dimethoxy-4-hydroxyphenyl) units were significantly acetylated whereas only traces of acetylated guaiacyl (4-hydroxy-3-methoxyphenyl) units could be detected.

How is it possible to establish whether monolignols are acetylated prior to the polymerization steps of lignification? Even finding acetylated monomers in lignifying tissues will not rigorously establish that they are involved in lignification. Structural analysis of the lignin polymer can provide a reasonably definitive answer. There is one lignification pathway that is significantly altered by pre-acetylation of the monolignols. That is the pathway in which the 9-OH on the monolignol becomes involved in post-coupling reactions, i.e. the pathway normally leading to 8–8-coupled (resinol) units **3**, Fig. 1. The key concept is the following. With the 9-position acetylated, 8–8-coupling can still presumably occur (the 9-OH is not required for the radical coupling step; the propenyl analog isoeugenol G-CH=CH-CH_3, for example, will also undergo 8–8-coupling), but the re-aromatization reactions following the radical coupling step can no longer be driven by the internal attack of the 9-OH on the quinone methide intermediate **QM2**, Fig. 1. The 9-acetylation prevents such a reaction. Other pathways must therefore be in effect producing other products. The important point is that the acetyl group can remain attached in non-resinol 8–8-coupling products, products that could not have arisen from post-coupling acetylation reactions.

Results and Discussion

In seeking preliminary evidence for sinapyl acetate incorporation, it didn't appear necessary to elucidate the full coupling and cross-coupling pathways for sinapyl acetate. All that was required was to show that sinapyl acetate **2**, in coupling and cross-coupling reactions, would give acetylated products that would produce DFRC′ 8–8-linked products identical to those that are released from

kenaf (lignins) and not from plants having non-acetylated lignins. Oxidation of sinapyl alcohol"**1** with H_2O_2/peroxidase or metal oxidants typically gives the lignan syringaresinol **3** as the predominant dehydrodimeric product, along with small amount of the 8–O–4-coupled product. In this study, sinapyl alcohol was oxidized with H_2O_2/peroxidase in a 20 mM buffer solution containing 20% acetone; syringaresinol **3** was the only 8–8-product, produced in over 90% yield. DFRC′ treatment of syringaresinol **3** yielded aryltetralin **6a**, Fig. 2, as a major product. Similar compounds are produced following thioacidolysis of 8–8-linked lignin units. Oxidation of sinapyl acetate **2** (Fig. 1) under similar conditions yielded a mixture of currently uncharacterized compounds retaining acetate groups. DFRC′ treatment of the mixture yielded **6c**, the diacetate analog of **6a** (from sinapyl alcohol). The structural analogy, from MS spectra (Fig. 2), indicates that sinapyl acetate also undergoes 8–8-coupling, and that at least one of the products **5** (Fig. 1, although the exact structure has not yet been determined) produces the aryltetralin **6c** following DFRC′ treatment. Oxidation of a mixture of sinapyl alcohol **1** and sinapyl acetate **2** must result in cross-coupling reactions to produce crossed 8–8-coupled structures **4**, since DFRC′ degradation now produces mono-acetylated aryltetralins **6b** in addition to the non- and di-acetylated analogs **6a** and **6c** (as evidenced by GC-MS).

It would be reasonable to expect that substructures **4** and **5** exist (in phenol-etherified form) in kenaf if sinapyl acetate participates in formation of its lignin. Selected ion chromatograms of TLC-fractionated DFRC′ products from kenaf lignin (Fig. 2) or whole kenaf cell walls clearly show the presence of all three DFRC′ products, compounds **6a-c**. Comparison of GC retention times and mass spectra of DFRC′ products with those from the *in vitro* coupling reactions of sinapyl alcohol and sinapyl acetate indicates that compounds **6b** and **6c** derive from sinapyl acetate. Compound **6a** derives from normal lignins, but the acetylated analogues **6b** and **6c** do not.

Although a great deal remains to be done to detail the coupling reactions, authenticate the nature and stereochemistry of the products, and fully elucidate their DFRC′ products, the preliminary data presented here appears to us to provide rather compelling evidence that sinapyl acetate is involved in lignification in kenaf, and is the likely source of the high 9-acetylation observed in kenaf bast fiber lignins. Detection of 9-acetates in syringyl 8–8-coupled DFRC′ products **6b-c** from kenaf suggests the existence of substructures which are likely formed from dehydrogenative coupling of sinapyl acetate itself or cross-coupling with sinapyl alcohol during the lignification process and provides evidence that acetates on kenaf lignin are formed through incorporation of sinapyl acetate, as a lignin precursor, into lignin macromolecules by radical coupling. Sinapyl acetate therefore appears to be an authentic lignin monomer in kenaf.

Conclusions

The preliminary evidence provided here that acylation is at the monolignol stage allows researchers to seek the substrates and presumed transferases involved in the specific acylation of monolignols, and to identify the genes responsible, allowing the process to be genetically manipulated.

The complete manuscript is available from our website at:
http://www.dfrc.ars.usda.gov/DFRCWebPDFs/2002-Lu-JCSCC-90.pdf

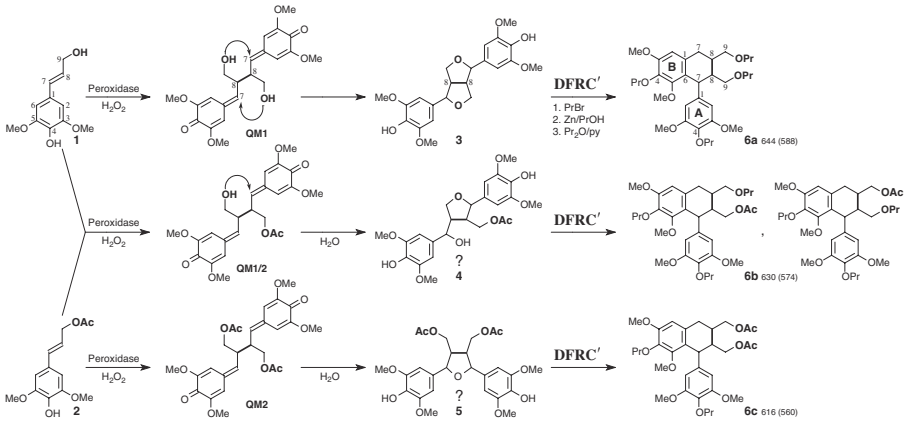

Fig. 1. The key to establishing whether monolignols are pre-acylated lies with the 8–8-coupling products (the resulting 8–8-bonds are bolded for emphasis). The traditional monolignol sinapyl al cohol **1** will dehydro-dimerize initially forming the 8–8-coupled bis-quinone methide intermediate **QM1**, which re-aromatizes by internal 9-OH attack on each quinone methide electrophilic 7-carbon to produce syringaresinol **3** as the overwhelmingly major product. When acylated sinapyl alcohol **2** dimerizes, it forms an analogous bis-quinone methide intermediate—**QM2**. However, **QM2** can not be re-aromatized by internal trapping. The products have not yet been characterized but it is logical that structure **5** would arise from water attack on one quinone methide moiety with the resulting 7-OH attacking the other quinone methide to form a tetrahydrofuran; analogous products have been found in ferulate dehydrodimers. When **1** and **2** radicals cross-couple, the intermediate bis-quinone methide **QM1/2** now has one quinone methide moiety which can be internally trapped by the single 9-OH to form a single tetrahydrofuran ring, but the other quinone methide can only be re-aromatized by attack of an external nucleophile. The resulting product, presumably **4**, therefore retains at most a single acetate. Products **6** result from DFRC′-degradation (the DFRC modification using only propionate reagents) of the non-, mono-, and di-acetylated 8–8-coupled units. See text for details. The MWs of DFRC′ products are given beside the compound numbers, with the MWs of the base peaks (used for Fig. 2) in bracket

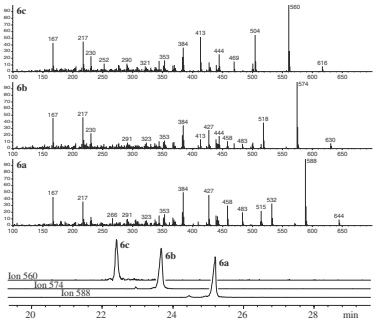

Fig. 2. Mass spectra and selected-ion chromatograms of DFRC products from kenaf showing the presence of aryltetralin products containing 0, 1, and 2 acetates.

Lignin Concentration in Plant Samples Determined by the Acetyl Bromide Soluble Lignin Spectrophotometric Method

R. S. Fukushima and R. D. Hatfield

Introduction

Lignin, a polyphenolic compound, inhibits the digestion of plant cell wall components, and this effect becomes more pronounced as the forage matures. For the understanding of how mechanistically lignin acts upon the cell wall carbohydrates it is imperative to determine its concentration with acceptable accuracy and precision. Most of the current methods for quantifying lignin are gravimetric. An alternative method has been proposed, which is based upon solubilization of lignin into a solution of 25% acetyl bromide in glacial acetic acid and reading it at 280 nm, the acetyl bromide soluble lignin (ABSL) method. The objective of this project was to compare lignin results obtained from the Klason lignin and ABSL methods of lignin quantification.

Materials and Methods

Plant materials included a range of forage plants and pine as a woody plant comparison (see Table 1). For the ABSL method procedure samples were incubated with 25% acetyl bromide in glacial acetic acid for 2h at 50° C, before diluting 20 fold in acetic acid and reading the absorbance at 280 nm. Isolated lignin used as standard was obtained through extraction with acidic dioxane (0.2NHCl-Dioxane). Klason lignin (KL) was the acid insoluble residue remaining after total hydrolysis with concentrated sulfuric acid of cell wall polysaccharides.

Results and Discussion

Lignins were extracted from the respective plants using HCl-dioxane and used as standards to develop regression equations to calculate lignin concentration in the original plant cell wall material. Table 1 shows the regression equation for each plant analyzed and the corresponding ABSL values.

As a general rule, regression slopes were similar at different maturity stages. The only exception was corn stalk that had a higher slope than all other samples (Table 1). It would appear that exchanges among some DL regression equations might be possible, therefore only one type of lignin (DL) isolate is necessary to use as a standard for determining lignin concentration in wide range of plants, regardless of origin, anatomical part or maturity stage. Once a regression curve is developed calibration will be required only occasionally. All intercepts but the one from corn stalk were close to zero.

Alfalfa and red clover lignin values determined through the ABSL method were lower than those obtained by the Klason's method. Pine showed higher concentration with the ABSL procedure (Table 1). The ratio between ABSL and KL were from 0.81 to 1.58 with legumes typically showing ratios below 1.0. This observation could be attributed to the hypothesis that Klason lignin method for legumes has some protein contamination and the ABSL method may account for any acid soluble lignin that otherwise would be lost during the strong acid digestion in Klason type lignin procedures.

Conclusion

The spectrophotometric procedure reported here employing dioxane-HCl lignin as a standard appears to be applicable to quantifying lignin concentration in a wide range of forage samples.

Table 1. Regression equations obtained from standard curves of DL preparations and lignin concentration (g kg^{-1} DM)[1] obtained through two analytical procedures

Sample name	Regression equation	ABSL	KL	ABSL/KL
Corn stalk	X = (Y' + 0.1244)/20.48	81.3	76.7	1.06
Alfalfa Y	X = (Y' + 0.0702)/17.20	99.7	123.0	0.81
Alfalfa M	X = (Y' + 0.0502)/17.15	127.9	130.4	0.98
Bromegrass	X = (Y' + 0.0709)/18.63	112.7	102.2	1.10
Bromegrass M1	X= (Y' +0.0981)/17.98	115.7	100.4	1.15
Bromegrass M	X = (Y' + 0.0981)/17.98	132.2	109.8	1.20
Red clover	X = (Y' + 0.0154)/16.13	63.1	71.2	0.89
Pine	X = (Y' + 0.0955)/17.747	404.7	256.0	1.58

[1]Values are means of two observations. Y – young; M – mature (1 and 2 refer to two different maturity stages); X – Concentration of ABSL (mg/mL); Y' – absorbance readings; ABSL – acetyl bromide soluble lignin; KL – Klason lignin.

Spectral Characteristics of Lignins Isolated with Acidic Dioxane

R. S. Fukushima and R.D. Hatfield

Introduction

Lignin is a complex phenolic polymer, composed of phenylpropanoid units and is present in forage cell walls. It is generally believed that lignin and its cross-linking to structural polysaccharides are the major impediments to fiber digestion. Spectrophotometric methods (e.g. the acetyl bromide soluble lignin method, ABSL) require isolation of lignin from the cell wall. Scanning of isolated lignins in a given spectral range provides clues for identifying variability in lignin composition and concentration. Also, the spectra are useful for evaluating the acetyl bromide soluble lignin method to determine if side reactions have occurred such as excessive degradation of carbohydrates or lignin.

Materials and Methods

Dioxane lignins were extracted from the cell wall of following plants; corn stalk, alfalfa, bromegrass, and loblolly pine using acidic dioxane (0.2 NHCl-dioxane). Dioxane lignins (DL) were dissolved in 25% acetyl bromide solution and heated for 2 hours at 50 °C before determining the spectral characteristics in the wavelength range of 250 to 350 nm. For comparison cell wall materials were treated with acetyl bromide (ABSL) method and the soluble lignin analyzed in the same spectral range.

Results and Discussion

Acetyl bromide soluble lignin spectral characteristics of DL extracts were similar to those of the original cell walls (Figure 1A and B). One would expect lignin to give similar spectra irrespective of the original source from which it is extracted since the major components that make up lignin macromolecules are the same (i.e., coniferyl and sinapyl alcohols). Acetyl bromide solubilized lignin should produce an absorbance maximum at 280 nm. If the lignin is unusually rich in syringyl units the maximum can be shifted slightly to 275 nm. The shoulders at 300 nm, evident in the grass samples, are due to hydroxycinnamates attached to the lignin.

Generally spectra from the different DL were similar. One exception was corn stalk DL standard that had a higher tracing than all other samples (Figure 1A). The deviation of the corn sample may be due to the unusually high levels of hydroxycinnamates, especially *p*CA attached to the lignin. This can be seen in the nitrobenzene products (data not shown) where *p*CA is the second largest component recovered. Such high levels of *p*CA could alter the acetyl bromide lignin spectrum. Although *p*CA has an absorption maximum 300-310 nm, it also has a strong shoulder at 280nm that would add to the lignin absorption maximum at 280 nm. Earlier work with milled-wood-enzyme lignins isolated from corn revealed that approximately 20% of this lignin fraction was made up of *p*CA. Bromegrass in this study had *p*CA levels that were one third those of corn.

Lignins isolated from cell walls using HCl-dioxane have nearly identical spectral characteristics as the lignin in the original cell walls. Such lignins provide good standards for calibrating spectrophotometric methods of determining lignin concentrations.

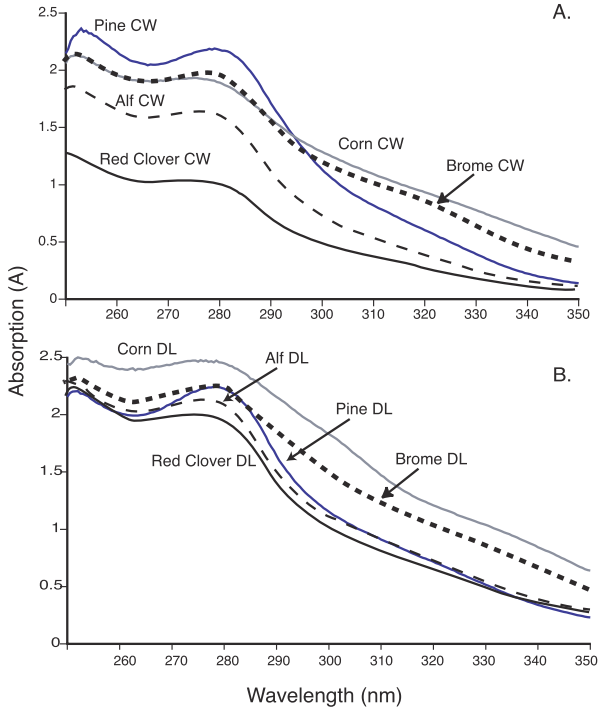

Fig. 1 Spectral characteristics of acetyl bromide soluble lignins. A. Acetyl bromide soluble lignin spectra obtained from isolated cell wall samples. B. Spectra obtained from dioxane-HCl extracted lignins used to produce standard curves of acetyl bromide soluble lignins.

Carbohydrate Profile in Two Isolated Lignins

R. S. Fukushima and R.D. Hatfield

Introduction

Lignin is a complex phenolic polymer forming an integral part of forage cell walls that cannot be digested by ruminants and often limits digestion of other wall components (i.e., carbohydrates and protein). Lignin concentrations must be determined with acceptable precision and accuracy in order to be useful as a predictor of nutritional value of forages. A method for measuring lignin in forages has been proposed which is based upon solubilization of lignin into a solution of 25% acetyl bromide in glacial acetic acid, the acetyl bromide soluble lignin (ABSL) method. Lignin is read at 280 nm; however, as with any spectrophotometric method, a reliable standard is needed to develop calibration curves. Among several options to extract and isolate lignin there is the acetyl bromide lignin (AcBrL) which employs the same acetyl bromide solution for ABSL and acidic dioxane lignin (DL) which employs dioxane acidified with 2 N HCl. This experiment was conducted to assess the type and amount of contaminants present in these two forms of lignin in order to asses their suitability as a standard.

Materials and Methods

The following plant materials were examined: corn stalk; alfalfa; bromegrass and loblolly pine. To prepare the cell walls, ground samples were sequentially extracted with water, ethanol, chloroform and acetone in a Soxhlet apparatus, until no color leached from the walls. Acetyl bromide reagent (25% AcBrin acolic acid, w/w) was used to solubilize lignin from plant cell walls. Lignin was recovered after neutralization and filtration. For comparison, lignin was isolated using 0.2 NHCl-dioxane reflux method. Neutral sugars, total uronosyls and total N were determined by general procedures.

Results and Discussion

AcBrL extraction method for obtaining lignin. Leaf tissue had higher concentrations of neutral sugars than the stems (Table 1). Total sugar concentration in the AcBrL varied from 1.44 to 36.92%. With the exception of pine, sugar contamination in AcBrL was high. Composition of individual neutral sugars was similar among the palnts with glucose (presumably from cellulose) being the highest. Protein content of AcBrL was considerable (Table 1).

DL extraction method for obtaining lignin. Utilization of acidic dioxane to extract and isolate lignin was tested to determine if this procedure would reduce the level of contamination, particularly carbohydrates. Uronosyl content of DL showed no differences among plants with the exception of pine. Neutral sugar concentration in DL showed a drastic reduction in sharp contrast to lignins obtained through extraction with acetyl bromide. The most prevalent sugar in the DL was xylose followed by arabinose and glucose which was a different profile from the AcBrL; sugar composition resembled that of hemicelluloses. Xylose was detected at higher concentration in grasses in comparison to alfalfa and pine. Other sugars exhibited no substantial trend to any species probably because the extraction conditions removed most of sugars such that quantity of the remaining sugars would be little enough to have any significant biological meaning. Apparently, there was no maturity effect on sugar composition. DL samples showed levels of protein varying from 9.5 to 71.5 g kg^{-1}

lignin; grasses exhibited lower concentration of protein than legumes and pine had the lowest content (Table 2).

Conclusions

These findings indicate that lignin extracted with acidic dioxane would be a better reference standard for lignin analysis by the acetyl bromide soluble lignin method.

Table 1. Total uronosyls, neutral sugars, individual composition of neutral sugars and protein content in the AcBrL (g kg^{-1} lignin)[1]

Sample name	Total uronosyls	Neutral sugars	Ara	Rha	Gal	Glc	Xyl	Man	Protein
Corn stalk	5.2	212.4	6.0	0	0.5	198.1	7.8	0	15.6
Alfalfa leaf	11.7	357.5	0.4	1.3	2.0	348.5	3.2	2.0	26.9
Alfalfa stem	18.8	158.6	0	0.4	0.4	156.5	1.3	0	33.6
Bromegrass leaf	7.3	352.3	7.5	0.2	0.5	340.8	3.3	0	18.0
Bromegrass stem	6.0	97.7	7.7	0	0	84.6	5.4	0	36.5
Pine	3.7	10.7	0	0	0	9.4	0	1.3	2.3

[1]Ara – arabinose; Rha – rhamnose; Gal – galactose; Glc – glucose; Xyl – xylose; Man – mannose.

Table 2. Total uronosyls, neutral sugars, individual composition of neutral sugars and protein in the dioxane lignin (g kg^{-1} lignin)[1]

Sample name	Uronosyls	Neutral sugars	Ara	Rha	Gal	Glc	Xyl	Man	Protein
Corn stalk	16.9	38.3	7.6	0.4	0.7	3.9	25.7	0	22.5
Alfalfa Y	12.4	22.8	1.9	0.5	1.4	2.4	16.6	0	71.5
Alfalfa M	12.5	19.6	0.9	0.5	1.2	2.6	14.4	0	41.7
Bromegrass Y	16.7	40.3	12.2	0	0.5	3.2	24.4	0	26.4
Bromegrass M1	14.5	34.1	11.5	0	0.2	2.7	19.7	0	34.2
Bromegrass M2	15.3	36.6	11.9	0	0.5	2.8	21.4	0	37.2
Pine	3.7	18.4	1.1	0	3.3	3.6	4.9	5.5	9.5

[1] Y – young; M – mature (1 and 2 refer to two different maturity stages).